

INTERNAL BALLISTIC DESIGN OPTIMIZATION OF A  
SOLID ROCKET MOTOR

A THESIS SUBMITTED TO  
THE GRADUATE SCHOOL OF NATURAL AND APPLIED SCIENCES  
OF  
MIDDLE EAST TECHNICAL UNIVERSITY

BY

SEVDA AÇIK

IN PARTIAL FULFILLMENT OF THE REQUIREMENTS FOR THE DEGREE OF  
MASTER OF SCIENCE  
IN  
MECHANICAL ENGINEERING

MAY 2010

Approval of the thesis:

**INTERNAL BALLISTIC DESIGN OPTIMIZATION OF A  
SOLID ROCKET MOTOR**

submitted by **SEVDA AÇIK**, in partial fulfillment of the requirements for the degree of **Master of Science in Mechanical Engineering Department, Middle East Technical University** by,

Prof. Dr. Canan ÖZGEN  
Dean, **Graduate School of Natural and Applied Sciences**

Prof. Dr. Süha ORAL  
Head of Department, **Mechanical Engineering**

Prof. Dr. Zafer Dursunkaya  
Supervisor, **Mechanical Engineering Dept., METU**

Dr. K.Atılgan TOKER  
Co-supervisor, **Roketsan Missiles Industries Inc.**

**Examining Committee Members:**

Prof. Dr. Faruk Arınç  
Mechanical Engineering Dept., METU

Prof. Dr. Zafer Dursunkaya  
Mechanical Engineering Dept., METU

Dr. K.Atılgan TOKER  
Roketsan Missiles Industries Inc.

Prof. Dr. M. Haluk AKSEL  
Mechanical Engineering Dept., METU

Uğur Ö. ARKUN, M.Sc.  
Roketsan Missiles Industries Inc.

**Date:** \_\_\_\_\_

**I hereby declare that all information in this document has been obtained and presented in accordance with academic rules and ethical conduct. I also declare that, as required by these rules and conduct, I have fully cited and referenced all material and results that are not original to this work.**

Name, Last name : Sevda AÇIK

Signature :

## **ABSTRACT**

### **INTERNAL BALLISTIC DESIGN OPTIMIZATION OF A SOLID ROCKET MOTOR**

Açık, Sevda

M. Sc., Department of Mechanical Engineering

Supervisor: Prof. Dr. Zafer Dursunkaya

Co-Supervisor: Dr. K.Atılğan Toker

May 2010, 66 pages

Design process of a solid rocket motor with the objective of meeting certain mission requirements can be specified as a search for a best set of design parameters within the overall design constraints. In order to ensure that the best possible design amongst all achievable designs is being achieved, optimization is required during the design process.

In this thesis, an optimization tool for internal ballistic design of solid rocket motors was developed. A direct search method Complex algorithm is used in this study. The optimization algorithm changes the grain geometric parameters and nozzle throat diameter within the specified bounds, finally achieving the optimum results.

Optimization tool developed in this study involves geometric modeling of the propellant grain, burnback analysis, a 0-dimensional ballistic performance

prediction analysis of rocket motor and the mathematical optimization algorithm. The code developed is verified against pretested rocket motor performance.

Key-words: Solid Rocket Motor, Grain Burnback, Internal Ballistics Design, Optimization, Complex Method

## ÖZ

### KATI YAKITLI ROKET MOTORLARI İÇİN İÇ BALİSTİK TASARIM OPTİMİZASYONU

Açık, Sevda

Yüksek Lisans, Makina Mühendisliği Bölümü

Tez Yöneticisi: Prof. Dr. Zafer Dursunkaya

Ortak Tez Yöneticisi: Dr. K.Atılğan Toker

Mayıs 2010, 66 sayfa

Katı yakıtlı roket motoru tasarım süreci; belirlenmiş misyon isteklerini sağlamak için, sistem kısıtları içinde en iyi tasarım parametrelerinin aranması olarak tanımlanabilir. Bulunabilecek olası çözümlerin içinden en iyisinin seçildiğinden emin olmak için tasarım sürecinde optimizasyon gereklidir.

Bu tez çalışmasında, katı yakıtlı roket motorları iç balistik tasarımında kullanılmak üzere bir optimizasyon aracı geliştirilmiştir. Bir “Doğrudan Arama Metodu (Direct Search Method)” olan Complex algoritmasını kullanan optimizasyon aracı; yakıt çekirdeği geometrik parametrelerini ve lüle boğaz çapını tanımlanan aralıklar içinde değiştirerek en iyi sonuca ulaşmaktadır.

Geliştirilen optimizasyon aracı; yakıt çekirdeğinin geometrik modellemesi, geriye yanma analizi, sıfır boyutlu iç balistik performans tahmini ve optimizasyon algoritmasını kapsamaktadır. Geliştirilen kod daha önce test edilmiş roket motoru sonuçları ile karşılaştırılarak doğrulanmıştır.

Anahtar Kelimeler: Katı Yakıtlı Roket Motoru, Geriye Yanma, İç Balistik Tasarım,  
Optimizasyon, Complex Metodu

## **ACKNOWLEDGEMENT**

I would like to express my deepest thanks and gratitude to Prof. Dr. Zafer DURSUNKAYA for his supervision and constant guidance through this study.

I would like to thank to my co-supervisor Dr. Kemal Atılğan TOKER, for his crucial advises and suggestions, he encouraged me to overcome the problems.

I would like to thank to Uğur ARKUN, for sharing his experience and for his great suggestions and aids throughout this study which help combining the mathematical work to real physics of the rocket propulsion.

I would like to express my sincere appreciation to my colleague Korhan COŞKUN for his crucial advises and invaluable efforts during the preparation of this thesis.

I would also like to thank to my friends Umut AKAY and Özlem SARCAN for their friendship and support.

Special thanks go to my mother Ayşe AÇIK and my entire family for always being there for me and giving me the motivation.

This thesis is dedicated to my family, without them nothing would have been made.

## TABLE OF CONTENTS

ABSTRACT .....	IV
ÖZ .....	VI
ACKNOWLEDGEMENT .....	VIII
LIST OF TABLES .....	XI
LIST OF FIGURES .....	XII
LIST OF SYMBOLS .....	XIV
LIST OF SYMBOLS .....	XIV
CHAPTERS .....	1
1 INTRODUCTION .....	1
1.1 LITERATURE SURVEY .....	1
1.1.1 Gradient Based Methods .....	3
1.1.2 Heuristic Methods .....	4
1.1.3 Hybrid Methods .....	5
1.2 SCOPE OF THE THESIS .....	6
1.3 CONTENTS OF THE THESIS REPORT .....	7
2 FUNDAMENTALS OF SOLID ROCKET MOTORISATION TOOL .....	8
2.1 CLASSIFICATION OF ROCKET MOTORS .....	8
2.2 SOLID PROPELLANT ROCKET MOTORS .....	9
2.2.1 Main Parts of Solid Propellant Rocket Motors .....	10
2.3 INTERNAL BALLISTICS DESIGN METHODOLOGY AND GOVERNING EQUATIONS .....	13
2.3.1 Ballistic Parameters .....	13
2.4 GRAIN BURNBACK ANALYSIS AND TYPICAL GRAIN CONFIGURATIONS .....	18
2.4.1 Grain Burnback Analysis .....	18
2.4.2 Typical Grain Configurations .....	21
3 SRM OPTIMIZATION TOOL .....	25
3.1 GENERAL .....	26

3.2	OPTIMIZER.....	29
	3.2.1 <i>Complex Method</i> .....	29
	3.2.2 <i>BCPOL Subroutine of IMSL</i> .....	31
3.3	BURNBACK.....	32
	3.3.1 <i>Burnback of End-Burning Grain</i> .....	32
	3.3.2 <i>Burnback of Internal Burning Grain</i> .....	32
	3.3.3 <i>Burnback of Star and Star-Tube Grain</i> .....	33
	3.3.4 <i>Burnback of Slot and Slot-Tube Grain</i> .....	33
3.4	BALLISTICS SOLVER.....	34
	3.4.1 <i>Assumptions</i> .....	34
	3.4.2 <i>Governing Equations</i> .....	35
3.5	OBJECT.....	38
4	VALIDATION.....	40
4.1	VALIDATION OF 0-D BALLISTIC SOLVER.....	40
	4.1.1 <i>Tubular Grain Performance Prediction</i> .....	40
	4.1.2 <i>Star Grain Performance Prediction</i> .....	42
4.2	VALIDATION OF OPTIMIZATION TOOL WITH KNOWN SOLUTIONS.....	44
	4.2.1 <i>Star Grain Optimization</i> .....	44
	4.2.2 <i>Slot-Tube Grain Optimization</i> .....	46
4.3	VALIDATION OF OPTIMIZATION TOOL AND COMPARISON WITH PREDESIGNED ROCKET MOTORS.....	49
	4.3.1 <i>Star Grain Optimization</i> .....	50
	4.3.2 <i>Slot-Tube Grain Optimization</i> .....	55
5	CONCLUSION AND DISCUSSION.....	61
	REFERENCES.....	63

## LIST OF TABLES

### TABLES

Table 3.1 Discrete and Continuous Parameters of Different Grain Types .....	27
Table 3.2 Continuous Parameters of Different Grain Types .....	28
Table 4.1 Geometric Parameters of Tubular Motor, Nondimensionalized Using the Throat Diameter .....	41
Table 4.2 Dimensionless Geometric Parameters of Star Motor (SM) .....	43
Table 4.3 Initial Guess and Bounds of Parameters of Optimization, SM Grain Dimensions and Optimized Solution .....	45
Table 4.4 Dimensionless Geometric Parameters of Slot-Tube Motor (STM) .....	47
Table 4.5 Initial Guess and Bounds of Parameters of Optimization, STM Grain Dimensions and Optimized Solution .....	48
Table 4.6 Dimensionless Initial Guess Parameters and Bounds of Star Grain Optimization .....	52
Table 4.7 Dimensionless Optimized Results for Star Grain .....	54
Table 4.8 Dimensionless Initial Guess Parameters and Bounds of Slot-Tube Grain Optimization .....	57
Table 4.9 Dimensionless Optimized Results for Slot-Tube Grain .....	59

## LIST OF FIGURES

### FIGURES

Figure 2.1 Main Parts of a Solid Propellant Rocket Motor .....	10
Figure 2.2 Burnback Analysis of a Slotted Grain Geometry .....	20
Figure 2.3 End-Burning Configuration.....	22
Figure 2.4 Internal-Burning Tube Configuration.....	22
Figure 2.5 Star Grain Geometry and Burnback Analysis [7].....	23
Figure 2.6 Slot Grain Configuration .....	24
Figure 2.7 Slot-Tube Configuration [15] .....	24
Figure 3.1 Optimization Tool Architecture .....	26
Figure 3.2 Illustration of a Simplex in Two and Three Dimensions [12].....	30
Figure 3.3 Zero-dimensional SRM Conservative Relations [26] .....	35
Figure 4.1 Tubular Motor.....	41
Figure 4.2 Comparison of Thrust-Time Histories of 0-D Ballistic Solver and Firing Test for TM .....	42
Figure 4.3 Comparison of Thrust-Time Histories of 0-D Ballistic Solver and Firing Test of SM.....	43
Figure 4.4 Comparison of Thrust-Time histories of Optimized Solution, Initial Guess and Objective for SM .....	46
Figure 4.5 Comparison of Thrust-Time histories of Optimized Result, Initial Guess and Objective for STM.....	49
Figure 4.6 Typical Thrust-Time Requirements of Solid Rocket Motors.....	50
Figure 4.7 Objective Thrust-Time Prepared for Optimization and SM Thrust-Time Curve.....	51
Figure 4.8 Comparison of Thrust-Time histories of Initial Guess for Different Number of Stars and Objective for Star Optimization.....	53
Figure 4.9 Comparison of Thrust-Time Histories of Initial Guesses and	

Optimized Results for Star Grain Optimization.....	54
Figure 4.10 Objective Thrust-Time Prepared for Optimization and Original STM's Thrust-Time Curve.....	56
Figure 4.11 Comparison of Thrust-Time histories of Initial Guess for Different Number of Slots and Objective .....	58
Figure 4.12 Comparison of Thrust-Time histories of Initial Guesses and Optimized Results for Slot-Tube Grain .....	59

## LIST OF SYMBOLS

$a$	Burning rate coefficient
$A_b$	Burning surface
$A_e$	Nozzle exit area
$A_t$	Nozzle throat area
$c^*$	Characteristic velocity,
$C_d$	divergence loss coefficient
$C_F$	Thrust coefficient
$D_{out}$	Outer diameter of propellant grain
$D_{port}$	Port diameter of propellant grain
$D_t$	Nozzle throat diameter
$D_{tip}$	Tip diameter for slot grain
$D_{tip-center}$	Tip-center diameter for slot grain
$F$	Thrust
$F_{max}$	Maximum Thrust
$F_{desired}$	Objective thrust
$F_{desired\_avg}$	Average objective thrust
$F_{iteration}$	Thrust of the iteration
$g_0$	Gravitational acceleration at sea level
$I_{sp}$	Specific impulse
$I_t$	Total impulse
$K$	Burning surface area to nozzle throat area ratio
$L$	Length of propellant grain
$L_{slot}$	Length of slot
$L_{star}$	Length of star
$\dot{m}$	Mass flow rate
$m_p$	Propellant mass

$m_{p_{\text{constraint}}}$	Propellant mass constraint
$M$	Mass stored in the chamber
$M_e$	Exit Mach number
$N$	Number of parameters
$n_{rb}$	Burning rate pressure exponent
$P$	Pressure
$P_{\text{amb}}$	Ambient pressure
$P_c$	Chamber pressure
$P_{c_{\text{max}}}$	Maximum chamber pressure
$P_{c_{\text{max\_constraint}}}$	Maximum chamber pressure constraint
$P_e$	Nozzle exit pressure
$r_1$	Fillet radius of star grain
$r_2$	Cusp radius of star grain
$r_b$	Propellant burning rate
$R$	Gas constant
$t$	Time
$t_b$	Burning time
$T$	Temperature
$v_e$	Velocity at nozzle exit

#### Greek Symbols:

$\rho$	density
$\gamma$	specific heat ratio
$\partial$	partial derivative operator
$\varepsilon$	Expansion ratio
$\varepsilon_f$	Convergence tolerance for complex method
$\sigma_p$	Temperature sensitivity of burning rate, % / ° K
$\pi_K$	Temperature sensitivity of pressure, % / ° K
$\xi$	Star angle

$\eta$  Star point semiangle

Subscripts:

SM Property of Star Motor

STM Property of Slot-Tube Motor

# **CHAPTER 1**

## **INTRODUCTION**

Design process of a solid rocket motor with the objective of meeting certain mission requirements can be specified as a search for a set of design parameters within the overall design constraints. A wide variation in the design parameters and the large number of possible combinations of these parameters turn this design process into a search with a very large number of possible answers.

In order to ensure that best possible design amongst all achievable designs is being acquired, optimization is essentially required during the design process.

### **1.1 LITERATURE SURVEY**

Finding the optimal design of a solid rocket motor to meet certain criteria has been subject of search since the 1960's. In 1980, Sforzini [1] commented in his own solid rocket optimization paper that despite the tractable mathematics involved in designing a solid rocket motor, "limited treatment of this subject appears in the literature". Today, Sforzini's statement is still true to a great extent [2]. Limited number of work can be found in open literature.

In 1968 Billheimer [3] acknowledged the importance of automating the design process of solid rocket motors in his paper. Although the physical modeling used in this study was limited by the computational resources available at the time, this paper was one of the first attempts at using an automated procedure [2].

Woltosz, [4] in 1977, proposes a pattern search technique (developed by Hook and Jeeves [5] ) to find an optimal solid grain geometry. He determines five critical design dimensions which maximize the total impulse - to motor weight ratio while meeting a specified minimum achieved velocity for a specific vehicle. [2]

Hook and Jeeves pattern search technique was also used by Foster and Sforzini [6] to minimize the differences between computed and desired solid rocket motor ignition characteristics based upon several igniter design parameters. Also In Sforzini's [1] 1980 paper, the pattern search technique was used to manipulate fifteen geometric variables governing the solid rocket motor design. Specified constraints were enforced by penalty functions in order to discourage unrealistic designs [2].

Swaminathan and Madhavan [7] tried to find the optimum propellant composition, which gives the highest possible specific impulse, using a direct random search technique, similar to simulated annealing.

In 1993 Clergen [8] developed a computerized expert system with which the designer can define design criteria such as minimum motor mass and obtain desired motor parameters for a certain mission. The system has a user-friendly, hypertext interface and the system basically uses past experience while selecting the motor design parameters. This system is built around a data base of known systems. [2]

McCain's [9] method is also an expert system in the sense that it is heuristic. This method combines a pattern search method with a heuristic system to develop rocket performance characteristics. The heuristic performs an independent design variable selection, and these design variables are then passed to the pattern search optimization package. The heuristic method then analyzes the effect of altering each independent SRM design variable and selects, based on gradient information, the variables to alter for the next design attempt. This technique, with its heuristic

sense, is an advancement of the pattern search technique of Sforzini, but still has some of the inherent weakness of any gradient-based method [2]

In 2001 Anderson et al.[2] used genetic algorithms to design solid rocket motors as a component within an overall missile system. In this study multiple goals, such as maximized range, minimized g-loading, minimized takeoff weight, and maximized fuel volume, are used to test the ability of genetic algorithms to work efficiently within a multidisciplinary framework.

Nisar and Guozhu presents a methodology for design optimization of wagon wheel grain [10] and for design optimization of SRM finocyl grain [11]. In both studies, they utilize a Hybrid Optimization (HO) technique by using Genetic Algorithm (GA) for global convergence integrated with Sequential Quadratic Programming for further local convergence of the solution thus attaining the final optimal solution.

As it can be seen in above examples, the methods used for optimization of solid rocket motors design fall into three broad categories: gradient based methods heuristic methods and hybrid methods

### **1.1.1 Gradient Based Methods**

Gradient based methods are numerical optimization algorithms which take a starting point and incrementally move in the direction that improves the objective function most. The most basic one of the gradient based minimization techniques is called the Gradient Descent Method. This method simply calculates the gradient of a function at each iteration and uses this as a search direction onto the next design point. This type of gradient-based method is a first order method, because it uses solely gradient information [12].

Other well-known gradient method, Newton's Method, is a second order one. This method is similar to the Gradient Descent method, but it adds second order information to its calculations in the form of the Hessian [12].

For constrained problems the most common algorithm is Sequential Quadratic Programming (SQP). This algorithm is the application of Newton's Method in the minimization of the Lagrangian of the constrained optimization model. Details of SQP and other gradient based algorithms can found in literature [13].

A major difficulty with gradient-based optimizers is dealing with noisy problems or problems containing many local minima. Given a response surface with various local minima, the algorithms will generally converge to the nearest local minima.

### **1.1.2 Heuristic Methods**

Heuristic methods are the optimization methods that use no gradient information and they are sometimes called gradient-free algorithms. *“A heuristic method applies a simple rule of thumb, often derived from natural processes, combined with some amount of stochasticity to an optimization problem”* [14]. In order to escape local extrema, most heuristic methods incorporate randomness. They can perform relatively well in non-convex, complex and noisy problems with both continuous and discrete design problems where gradient based methods have difficulty. But heuristic methods are still not guaranteed to find the global optimum [14].

The simplest derivative-free method is the one referred to as Direct Search. This method could be named random search, in that it merely checks objective function values, and accepts good points and rejects bad points, ending when a maximum iteration number has been achieved. Through the years more and more sophisticated logic has been developed to allow these types of algorithms to intelligently search through the design space. These may be as simple as

distributing the search, such as in Parallel Direct Search [15], or using a simplicial method, as in Box's Complex Method [16]. One of the more interesting methods developed recently, is Jones' Direct method, which employs a bounding technique performing Lipschitz optimization without the Lipschitz constant [17].

Other important derivative-free methods are Simulated Annealing and Genetic Algorithms. These methods are rather heuristic and do not use gradients. Genetic algorithms use the basic evolution strategy of natural selection which is a biological process in which the 'fittest' individual tend to survive, thereby optimizing the population. A genetic algorithm works with a population of individual design points, rather than optimizing a single point design like a gradient-based method [14].

### **1.1.3 Hybrid Methods**

Hybrid methods use a combination of gradient-based methods and Heuristic methods. An example of hybrid method is to use a heuristic method to move towards a global solution area, and switch to a second order gradient-based method to quickly move towards the final solution [12]. Therefore hybrid optimization methods utilizes advantages of both gradient-based methods and heuristic methods by combining the speed of local optimization with the robustness of global optimization.

## 1.2 SCOPE OF THE THESIS

The purpose of this study is to develop an internal ballistic design optimization tool for solid rocket motors. For a given objective, in this case objective thrust-time curve of the rocket motor, optimization tool yields the optimum propellant grain geometry and nozzle geometry. This optimization process will aid the solid rocket motor design engineer in making the best initial design selections and thereby reducing the overall "design cycle time" of a project.

Optimization tool developed in this study, involves geometric modeling of the propellant grain, burnback analysis, ballistic performance prediction analysis of solid rocket motor and the mathematical optimization algorithm.

Six types of propellant grain geometries are involved in this study; end burning, internal burning tube, slot, slot-tube, star and star-tube grain geometries. Burnback analysis is conducted by using analytical methods. For the performance prediction of a rocket motor, a 0-D internal ballistic solver is developed and used. Optimization is obtained using a direct search technique "complex method". The objective function to be optimized or minimized is the summation of the squares of the differences between the desired and computed thrust values of the SRM at specified times during motor operation divided by the average desired thrust and total number of data. Specified constraints on propellant weight and chamber pressure are enforced by penalty functions in order to discourage unrealistic and/or undesired designs.

The developed optimization tool, which is described in this thesis, is validated with the results of previously designed rocket motor data and actual firing test data .

### **1.3 CONTENTS OF THE THESIS REPORT**

In Chapter 2, a background on fundamentals of solid rocket motors is given. Classification of rocket motors, solid propellant rocket motor fundamentals, internal ballistic design methodology and governing equations, grain burnback analysis and typical grain configurations are presented in this chapter.

Chapter 3 contains the detailed description of the optimization tool and its subprograms. Optimization tool is composed of subprograms OPTIMIZER, BURNBACK, BALLISTIC SOLVER and OBJECT. Every subprogram has a different function. The methodology used and their governing equations are presented in this chapter.

Validation of the tool and the results are presented in Chapter 4. Test cases involving pretested rocket motor results are implemented.

## CHAPTER 2

### FUNDEMENTALS OF SOLID ROCKET MOTORS

#### 2.1 CLASSIFICATION OF ROCKET MOTORS

Rocket motors are widely used to impart a desired velocity to a flight vehicle which requires high thrust in order to transport its payload. A rocket motor is a typical energy transfer system. The chemical energy inside the fuel is converted to the thermal energy by a combustion process. High pressure and high temperature combustion product gases are expanded through a converging-diverging nozzle [18]. By this process “*internal energy of the gas is converted into kinetic energy of the exhaust flow and the thrust is produced by the gas pressure on the surfaces exposed to the gas*” [19].

Rocket motors are classified in many ways. The most common way is the classification according to the physical state of the propellant [18]. These are as follows:

a) *Solid Propellant Rocket Motors (SRM)*: As its name implies, the propellant of the motor is in the solid state. The oxidizer and the fuel is premixed and is contained and stored directly in the combustion chamber. Since the solid propellant both includes fuel and oxidizer, solid propellant rocket motors can operate in all environmental conditions. In comparison to other types of rockets, solid propellant rocket motors have simple design, , are easy to apply and require little or no maintenance [20].

b) *Liquid Propellant Rocket Motors*: This type of rocket motors use liquid propellants that are fed under pressure into the combustion chamber. In the chamber, the liquid fuel and oxidizer are mixed and burned to form hot gaseous products. Some liquid propellant rocket motors are capable of repetitive operation, that is they can be started and shut off at will. Also the thrust level can be adjusted during operation. The main disadvantage of a liquid rocket propulsion system is that; it requires several precision valves and a complex feed mechanism which includes, a relatively complex combustion chamber and propellant pumps, turbines, or a propellant-pressurizing device [18], [20].

c) *Gaseous Propellant Rocket Motors*: Gaseous propellant rocket motors use a stored high pressure gas as their working fluid or propellant. They are much like the liquid propellant rocket motors. Since the stored gas requires relatively larger and heavier tanks and since they require complex feed mechanisms, gaseous propellant rocket motors are the least used type of rocket motors [18], [21].

d) *Hybrid Rocket Motors*: In hybrid rocket motors usually the fuel is in solid state and the oxidizer is in liquid phase. In this hybrid motor concept, oxidizer is injected onto the solid fuel grain inside the combustion chamber. Like the liquid propellant rocket motors hybrid motors can be started and shut off at will. Hybrid motors have lower density-specific impulse than solid propellant systems [18].

## **2.2 SOLID PROPELLANT ROCKET MOTORS**

When compared to other types of rocket motors, solid propellant rocket motor (SRM) is the most commonly used one due to its relatively simple design, high reliability, ease of manufacture and cheapness. SRM can be used for a wide variety of applications requiring wide range of magnitude (few Newtons to several million Newtons) and duration of thrust [21].

The schematic diagram of a solid propellant rocket motor is shown in Figure 2.1

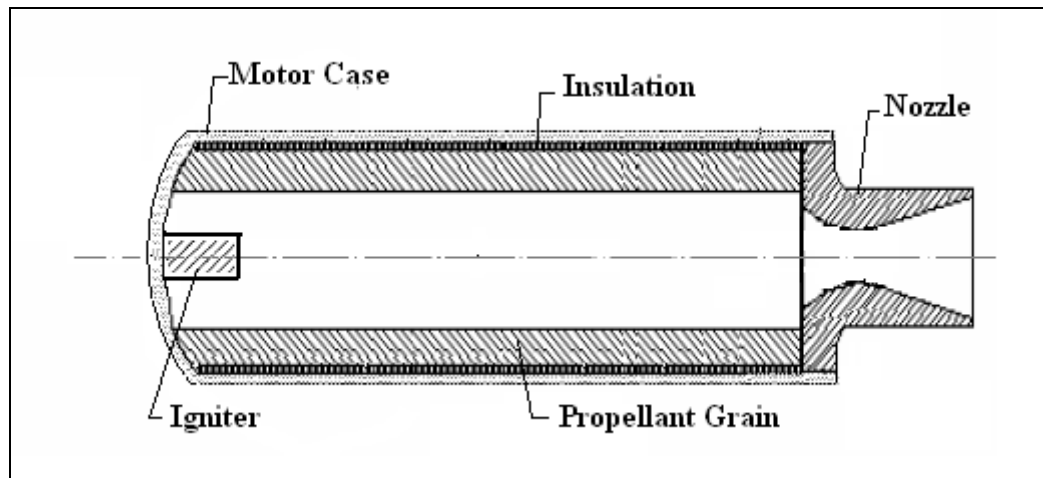


Figure 2.1 Main Parts of a Solid Propellant Rocket Motor

As shown in the figure above, SRMs are mainly composed of a motor case, an igniter, a nozzle, propellant grain and insulation.

## 2.2.1 Main Parts of Solid Propellant Rocket Motors

### 2.2.1.1 Motor Case

Generally motor case is a cylindrical cover containing the solid propellant, igniter and insulator. The combustion takes place in the motor case; therefore, sometimes it is referred to as combustion chamber.

The case must be capable of withstanding the internal pressure resulting from the motor operation, approximately 3-30 MPa, with a sufficient safety factor. Therefore motor case is usually made either from metal (high-resistance steels or high strength aluminum alloys) or from composite materials (glass, kevlar, carbon) [22]. In addition to the stresses due to the pressure in the chamber, thermal stresses

may sometimes be critical and, when the case also serves as flight vehicle body, bending loads and inertial forces also play an important role in determining the thickness and the material of the motor case.

#### **2.2.1.2 Insulation**

High temperature of the combustion gases, ranging from approximately 2000 to 3500 K, requires the protection of the motor case or other structural subcomponents of the rocket motor. Typical insulator materials have low thermal conductivity, high heat capacity and usually they are capable of ablative cooling. Most commonly used insulation materials are EPDM (Ethylene Propylene Diene Monomer) with addition of reinforcing materials.

#### **2.2.1.3 Igniter**

The ignition system gives the energy to the propellant surface necessary to initiate combustion. Ignition usually starts with an electrical signal. The ignition charge have a high specific energy, they are designed to release either gases or solid particles. Conventional heat releasing compounds are usually pyrotechnic materials, black powder, metal-oxidant formulations and conventional solid rocket propellant [20].

#### **2.2.1.4 Nozzle**

High temperature, high pressure combustion gases are discharged through the converging-diverging nozzle. By this way, chemical energy of the propellant is converted to kinetic energy and thrust is obtained. The geometry of the nozzle directly determines how much of the total energy is converted to kinetic energy. Therefore nozzle design has a very important role on the performance of a rocket motor [21].

Nozzles are usually classified according to their structural mounting technique or the shape of the contour; such as submerged nozzle, movable nozzle and bell-shaped nozzle.

Combustion product gases have an erosive effect with their high temperature and high velocity and also with a high concentration of liquid and solid particles like metal oxides inside them. Material selection of the nozzle is a very important step of nozzle design, especially for the throat region where erosive effects are more dominant. Refractory metal, carbon containing composites or graphite and reinforced plastic that will withstand erosive effects are commonly used as throat material.

#### ***2.2.1.5 Propellant Grain***

Solid propellant is cast in a certain configuration and geometry that is called the propellant grain.

The propellant grains can be subcategorized into two main configurations; case-bonded grain and free-standing grain. Case-bonded grains are directly cast into the motor case already provided with thermal insulation. After the curing operation the propellant grain is completed, this motor case with the propellant grain is ready to be mounted with the other components of the motor. Free standing grains are not directly cast into the motor case, instead the propellant is cast in some special mold. When the cure process of the propellant is completed, the grain is extracted from this mold. Free standing grains are loaded to the insulated motor case on the assembly line, that is why they are sometimes called as cartridge-loaded grains.

Burning surface of the grain changes during motor operation as the propellant burns. Burnback analysis determines this change in the grain geometry. The

geometric design of the grain ultimately defines the performance characteristics that can be obtained with a given propellant type and nozzle.

## **2.3 INTERNAL BALLISTICS DESIGN METHODOLOGY AND GOVERNING EQUATIONS**

The mission requirements of a specific flight vehicle system are usually the desired range, time of flight and velocity of the system in operation. For the rocket motor side, all these requirements can be simplified to the thrust time history of the rocket motor with some geometrical constraints. The thrust time curve characteristics depend on the combustion features propellant properties, grain geometry, and nozzle design. The branch of applied science describing these is known as internal ballistics [1].

The objective of the internal ballisticians is to provide the rocket motor a propellant grain that will evolve combustion products consistent with the thrust-time schedule required for the mission. In order to achieve this objective, the designer deals with some parameters of the rocket motor, called ballistic parameters. Some of these ballistic parameters are explained in the following sections.

### **2.3.1 Ballistic Parameters**

#### ***2.3.1.1 Nozzle Throat Area and Expansion Ratio***

The flow area at the nozzle throat  $A_t$  is a very important design parameter of nozzle. It is evaluated in conjunction with the variables associated with thrust coefficient, nozzle exit diameter, ambient pressure, chamber pressure and nozzle inefficiencies.

Nozzle expansion ratio is defined as the ratio of nozzle exit area to the nozzle throat area as given below [1]. The expansion ratio for the optimum expansion can be calculated by using this isentropic formula as given below.

$$\frac{A_t}{A_e} = \left[ \frac{\gamma + 1}{2} \right]^{\frac{1}{\gamma-1}} \left[ \frac{P_e}{P_c} \right]^{\frac{1}{\gamma}} \sqrt{\frac{\gamma + 1}{\gamma - 1} \left[ 1 - \left[ \frac{P_e}{P_c} \right]^{\frac{\gamma-1}{\gamma}} \right]} \quad (2.1)$$

$$\varepsilon = \frac{A_e}{A_t} \quad (2.2)$$

### 2.3.1.2 Thrust Coefficient

Thrust coefficient  $C_F$  is defined as the thrust divided by the chamber pressure and the throat area  $A_t$ . Physically  $C_F$  is an expression for efficiency of the nozzle for a fixed propellant configuration.

The thrust coefficient  $C_F$  is a function of gas property  $\gamma$ , nozzle expansion ratio  $\varepsilon$ , the pressure ratio across the nozzle  $P_c/P_e$  and the pressure outside the nozzle  $P_{amb}$  [18].

$$C_F = \sqrt{\frac{2\gamma^2}{\gamma - 1} \left[ \frac{2}{\gamma + 1} \right]^{\frac{\gamma+1}{\gamma-1}} \left[ 1 - \left[ \frac{P_e}{P_c} \right]^{\frac{\gamma-1}{\gamma}} \right]} + \frac{P_e - P_{amb}}{P_c} \varepsilon \quad (2.3)$$

The relation between  $C_F$ ,  $P_c$ ,  $A_t$  and thrust  $F$  is given by the following equation;

$$C_F = \frac{F}{P_c A_t} \quad (2.4)$$

### 2.3.1.3 Burning Rate

Propellant grain burns in a direction perpendicular to the grain surface. The rate, at which a propellant burns, usually described by a reference value at a specific pressure [23]. Such value is called burning rate and its unit is meters per second. As an independent parameter, the burning rate is one of the propellant properties.

Aside from the propellant formulation and propellant manufacturing process, burning rate in a full-scale motor can be increased by the following [18]:

1. Combustion chamber pressure.
2. Initial temperature of the solid propellant.
3. Combustion gas temperature.
4. Velocity of the gas flow parallel to the burning surface.
5. Motor motion (acceleration and spin-induced grain stress).

The relation between burning rate and the chamber pressure is governed by the following empirical equation, also known as Saint Robert's burn rate law:

$$r_b = a.P_c^{n_{rb}} \quad (2.5)$$

This empirical expression defines the burning rate of the propellant; values  $a$  and  $n$  usually derived from strand burner tests or small subscale burning rate test motor firings at different operating pressures

The sensitivity of burning rate to propellant temperature can be expressed in the form of temperature coefficients, the two most common are;

$$\sigma_p = \frac{1}{r_b} \left[ \frac{\partial r_b}{\partial T} \right]_P \quad (2.6)$$

$$\pi_K = \frac{1}{P} \left[ \frac{\partial P}{\partial T} \right]_K \quad (2.7)$$

where  $\sigma_P$  is known as the temperature sensitivity of burning rate expressed as percent change of burning rate per degree change in propellant temperature at a particular value of chamber pressure. The second one  $\pi_K$  is known as the temperature sensitivity of pressure expressed as percent change of chamber pressure per degree change in propellant temperature at a particular value of K which is the ratio of the burning surface area to throat area [18].

#### **2.3.1.4 Characteristic Velocity:**

Characteristic velocity  $C^*$  is a function of the propellant characteristics and combustion chamber design; it is independent of nozzle characteristics. The  $C^*$  is used in comparing the relative performance of different chemical rocket propulsion system designs and propellants; it is easily determined from measured data of  $\dot{m}$ ,  $P_c$ , and  $A_t$ . The  $C^*$  can be formulated as [18]

$$C^* = \frac{P_c A_t}{\dot{m}} \quad (2.8)$$

#### **2.3.1.5 Thrust**

The thrust of a SRM is the force produced by a rocket propulsion system acting upon a vehicle. In a simplified way, it is the reaction experienced by its structure due to the ejection of matter at high velocity. The thrust is the main design constraint of a propulsion system.

Thrust can be calculated from momentum equation applied on the overall rocket system ;

$$F = \dot{m}v_e + (P_e - P_{amb})A_e \quad (2.9)$$

In terms of other ballistic parameters F can be defined as

$$F = C_F P_c A_t \quad (2.10)$$

### 2.3.1.6 Specific Impulse and Total Impulse

Specific impulse,  $I_{sp}$ , is a measure of the impulse or momentum change that can be produced per unit mass of the propellant consumed. Specific impulse, on the other hand, can be described as the ratio of the motor thrust to mass flow rate and hence its value is very important in the determination of the propellant weight necessary to meet the ballistic requirements [23]. Specific impulse is defined as

$$I_{sp} = \frac{c^* C_F}{g_0} = \frac{F}{\dot{m}g_0} \quad (2.11)$$

The total impulse is the thrust force F integrated over the burning time t.  $I_t$  is directly proportional to the total energy released by all the propellant of the propulsion system [18].

$$I_t = \int_0^t F dt \quad (2.12)$$

For constant thrust and negligible start and stop transients this reduces to

$$I_t = Ft \quad (2.13)$$

### **2.3.1.7 Chamber Pressure and MEOP**

Chamber pressure is the gas pressure inside the combustion chamber during motor operation. In grain design process, usually a limit on maximum pressure is established at the time grain design activity commences. Concurrent with grain design, the motor case and other structural components are being designed and analyzed with this maximum pressure [18]. This constraint on chamber pressure is usually named as “Maximum Expected Operating Pressure” (MEOP).

## **2.4 GRAIN BURNBACK ANALYSIS AND TYPICAL GRAIN CONFIGURATIONS**

### **2.4.1 Grain Burnback Analysis**

Burning surface of the grain changes during motor operation as the propellant burns. Burnback analysis determines this change in the grain geometry. As the burning surface changes chamber pressure and the thrust of the rocket motor changes, therefore performance of the motor is directly related to burnback steps of the propellant.

Grain burnback is a pure geometrical analysis. The geometry deforms regardless of the thermal effects or flow inside the chamber (except for some special cases like erosive burning) The burning surface at each point recedes in the direction normal to the surface at that point [18].

Data obtained from burnback analysis is a relationship between burning surface and web distance burned, usually web burnt vs. burning surface, is an input for the internal ballistic performance prediction. This data obtained from burnback analysis almost entirely depends on the initial shape of the propellant grain

Analytical methods, numerical methods and drafting techniques are commonly used in grain burnback analysis.

#### ***2.4.1.1 Analytical Methods***

In these methods, usually the dimensional parameters are adapted for every burn step and the burning surface is calculated analytically at each burn step [21]. Several analytical methods for 2-D grain geometries in literature [24], [25], [26] have been reported.

The Solid Propellant Rocket Motor Performance Computer Program (SPP) is a popular SRM internal ballistics simulation software (developed in USA) with three available analytic methods for grain design and evolution: two-dimensional, axisymmetric, and three-dimensional. In axisymmetric and three dimensional cases, initial port geometry was defined through the use of a series of bounding surfaces composed of primitive shapes, such as; cylinders, cones, prisms or spheres [27].

#### ***2.4.1.2 Numerical Methods***

In these methods, numerical algorithms are used in order to evaluate the propellant grain surface regression. These methods do not need to divide the grain geometry into simple solids, complex geometries can be modeled and burnback analysis can easily be performed. Main disadvantages of such methods are the numerical errors involved and high computation time required for analysis [21]. Several different applications of numerical methods in burnback analysis can be found in literature [28], [29], [30], [31].

### 2.4.1.3 Drafting Techniques

Drafting tools can be used for both two-dimensional and three-dimensional grain burnback analysis.

In two dimensional analysis cross-section of the initial propellant grain is modeled using a CAD software program. After modeling the initial geometry, it can be offset by equal distances to obtain the burnback steps. Burning area at each step can be found by multiplying each perimeter with length of the grain. Burnback analysis of a slot geometry is shown in Figure 2.2. In this analysis only one half of a slot part is involved since the geometry is symmetric. The total burning area can be found by multiplying the result for one slot with total number of slots.

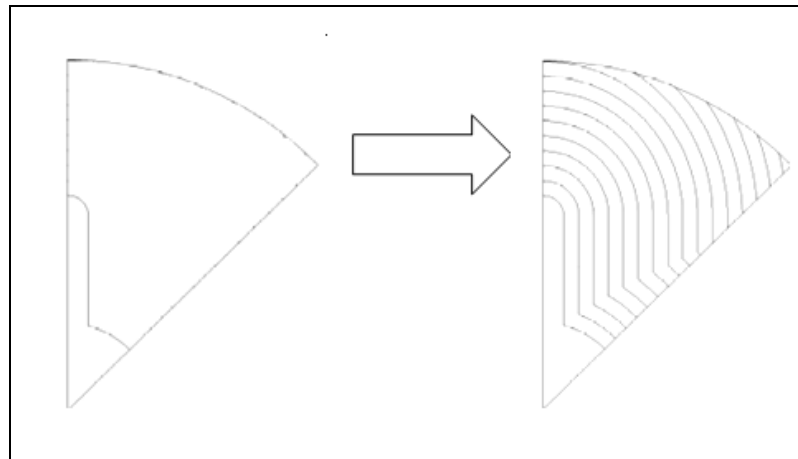


Figure 2.2 Burnback Analysis of a Slotted Grain Geometry

In three-dimensional analysis solid model of the propellant grain at the beginning of the operation is modeled parametrically. Most of the commercial CAD programs such as I-DEAS, Unigraphics NX, AutoCAD Mechanical Desktop (AMD) allow parametric modeling. Then the parameters that change during the burnback process can be changed or every burn step. This parameterization can be done either to the complete grain geometry or the grain geometry can be divided into simpler geometries before the parameterization process [21].

## 2.4.2 Typical Grain Configurations

For different system missions, different thrust-time profiles are required for rocket motors such as progressive, neutral or boost and sustain. By changing the propellant grain configuration, different thrust time profiles can be obtained from a rocket motor. Grain configurations can be categorized in several ways [23];

- Inner geometry of the grain (Star, wagon, internal burning tube etc.)
- Outer shape of the grain (Tubular, spherical any other unconventional shape)
- The propellant used (single propellant grain, dual propellant grain)
- the dimensional analysis (two-dimensional grain, three-dimensional grain)

Details of the most commonly used grain configurations in SRM applications are given in the subsequent sections.

### 2.4.2.1 *End-Burning Grain*

End-burning grain (Figure 2.3) geometry is the simplest configuration. It is distinguished from all other configurations by the orientation of burning which is totally in the longitudinal direction. Burning surface for such a grain geometry is defined by the end area and it is ideally constant during the motor operation, yielding a neutral thrust-time curve. In its simplest form the end burning grain is defined by two variables, length  $L$  and diameter  $D$ . End burners typically are applicable to missions requiring relatively long durations and low thrust level [23].

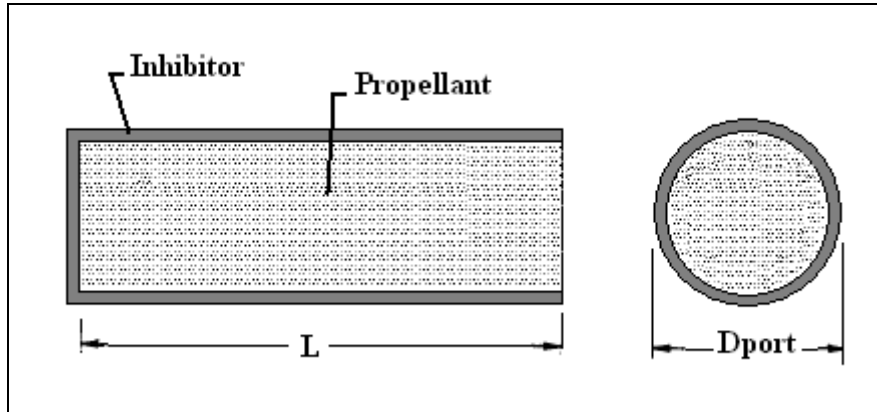


Figure 2.3 End-Burning Configuration

#### 2.4.2.2 Internal-Burning Tube (Tubular) Grain

The internal-burning tube is one of the most practical and preferred configurations. It is a radially burning grain with ends usually unrestricted, otherwise it burns progressively [23]. It is typically case-bonded which inhibits the outer surface. The internal-burning tube is defined by a length  $L$  and two diameters  $D$  and  $D_{port}$ . These parameters determine the trend (progressive, neutral or regressive) of the thrust-time curve of internal-burning tube grain.

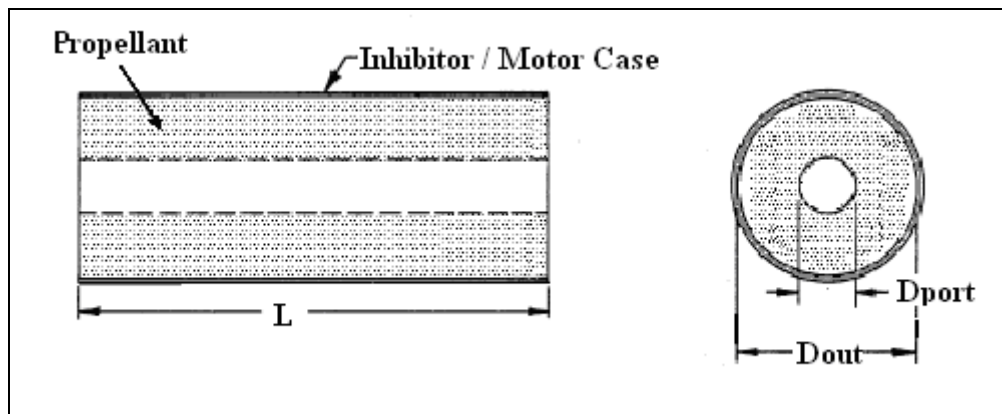


Figure 2.4 Internal-Burning Tube Configuration

### 2.4.2.3 Star Grain

The star geometry is a radially burning cylindrical with distinctive geometric properties (Figure 2.5). Seven independent geometric variables defined in Figure 2.5 characterize the star geometry;  $D_{out}$ ,  $r_1$ ,  $r_2$ ,  $\omega$ ,  $\eta$ ,  $\xi$ ,  $N$ .

The trust time profile of a star shaped grain can be regressive, neutral or progressive depending on the parameters defining the geometry.

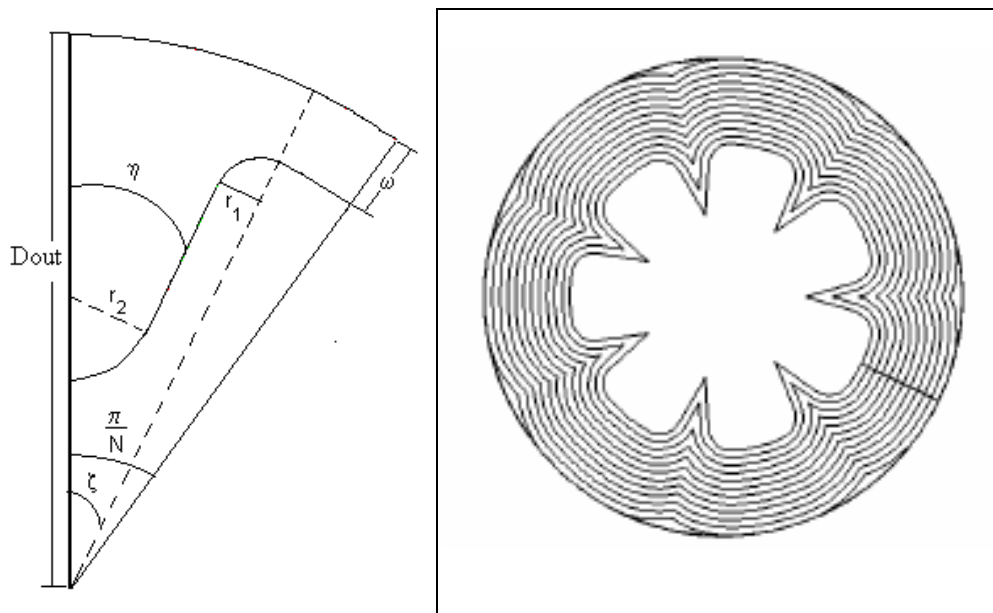


Figure 2.5 Star Grain Geometry and Burnback Analysis [7]

### 2.4.2.4 Slot Grain

The slot grain is essentially a special case of the star grain with the points “bored out” [24] as shown in Figure 2.6. There are five independent parameters of slot configuration;  $R_{out}$ ,  $R_{port}$ ,  $R_{tipcenter}$ ,  $I_t$ ,  $N$ .

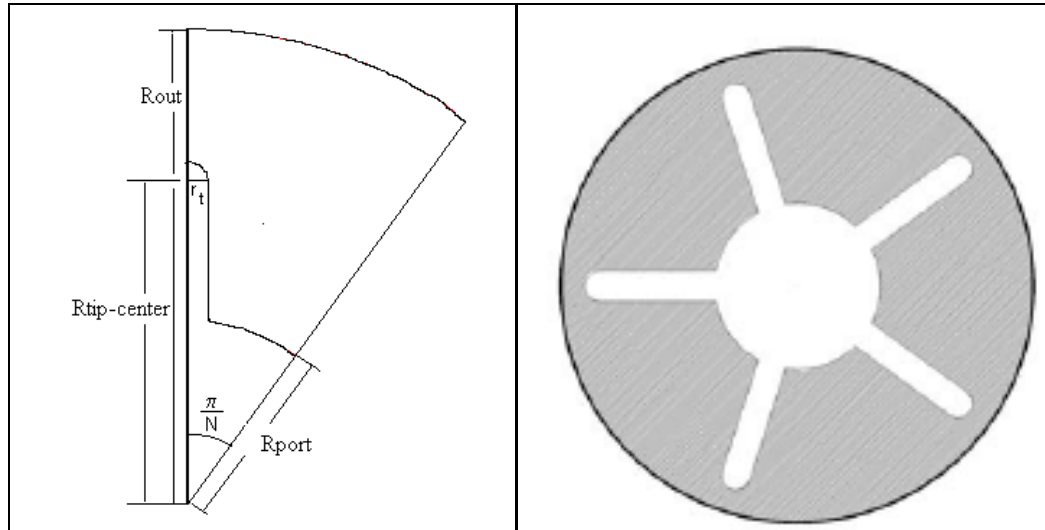


Figure 2.6 Slot Grain Configuration

#### 2.4.2.5 Slot-Tube or Star-Tube Grain

Above mentioned geometries were two dimensional geometries, that is the cross sectional shape of these grains are constant from head end to aft end. These geometries are not very useful for dual level of thrust (boost and sustain) [21]. For dual level of thrust or applications where neutrality is essential and sliver is, slot-tube or star-tube configurations are used. These geometries are simply composed of two different geometries attached together; usually a cylinder (internal-burning tube) and a star or slot. In literature these geometries are sometimes mentioned as “Finocyl geometry”. The word finocyl comes from the phrase “fins on a cylinder” [21]. Slot-Tube configuration is shown in Figure 2.7.

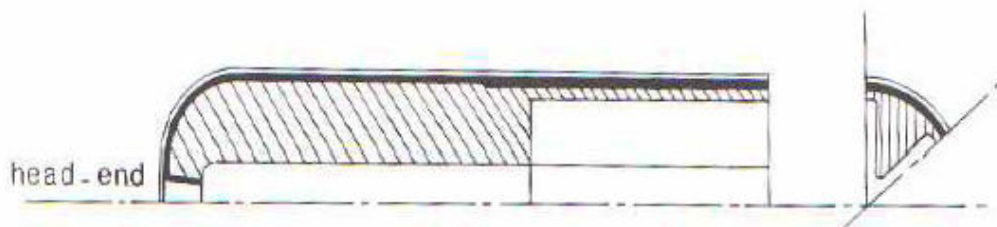


Figure 2.7 Slot-Tube Configuration [15]

## **CHAPTER 3**

### **SRM OPTIMIZATION TOOL**

In this chapter, internal ballistics design optimization tool developed for solid rocket motors will be presented.

Optimization tool developed in this study, involves geometric modeling of the propellant grain, burnback analysis, ballistic performance prediction analysis of rocket motor and the mathematical optimization algorithm.

Six types of propellant grain geometries are involved in this study; end burning, internal burning tube, slot, slot-tube, star and star-tube grain geometries. Burnback analysis is conducted by using analytical methods. For the performance prediction of rocket motor, a 0-Dimensional internal ballistics solver is developed and used. Optimization is obtained using a direct search technique “complex method”. The object function to be optimized or minimized is the summation of the squares of the differences between the desired and computed thrust values of the SRM at specified times during motor operation divided by the average desired thrust and total number of data. Specified constraints on propellant weight and chamber pressure are enforced by penalty functions in order to discourage unrealistic and/or undesired designs.

### 3.1 GENERAL

This optimization tool is based on the conventional architecture of an optimization program. Every subprogram has a different function and can easily be separated from the optimization subprogram, OPTIMIZER.

This architecture (Figure 3.1) provides capabilities to change any subprogram in order to compare other programming algorithms. Each subprogram is explained in detail in the following sections.

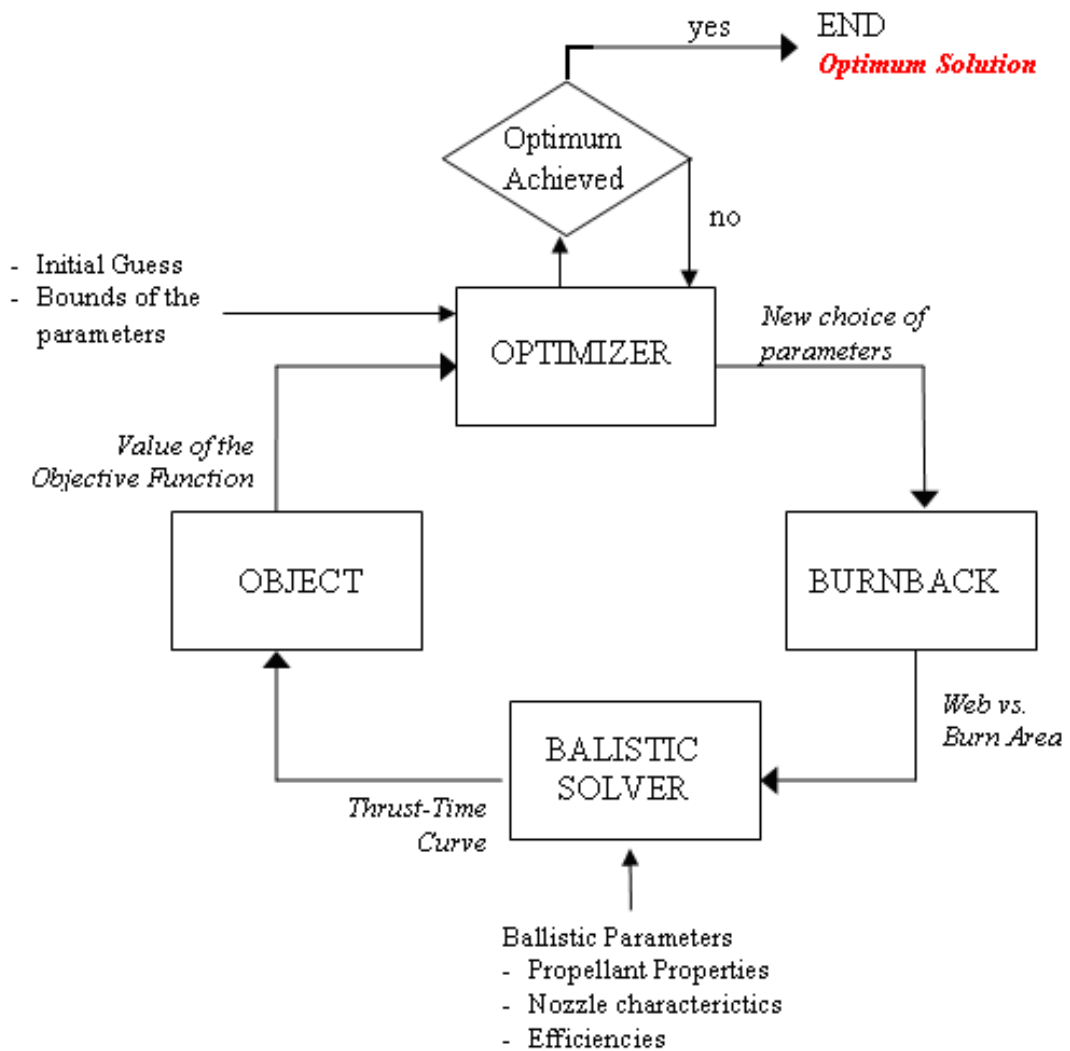


Figure 3.1 Optimization Tool Architecture

Variable parameters of solid rocket motor design involved in this study can be divided into two groups; continuous parameters and discrete parameters. Continuous parameters such as grain diameter or grain length can change continuously in the solution domain. Discrete parameters such as “grain type” and “number of slot or star points(N)” can not change continuously. OPTIMIZER subprogram does not deal with discrete parameters. For a set of discrete parameters optimum values of continuous parameters are found by OPTIMIZER, then iteration starts again for other set of discrete parameters. For each set of discrete parameters, optimization is performed separately and then all the results are compared to find the optimum solution.

Six different grain geometries are involved in this study. Number of continuous (n) and discrete parameters changes for each grain type as shown in Table 3.1 . These parameters were depicted in figures of each grain type in section 2.4.2. Also definition of each parameter is given in Table 3.1

Table 3.1 Discrete and Continuous Parameters of Different Grain Types

Discrete Parameters	END-BURN	TUBULAR	STAR	STAR-TUBE	SLOT	SLOT-TUBE
	-	-	# of Stars N (3-20)	# of Stars N (3-20)	# of Slots N (3-20)	# of Slots N (3-20)
Continuous Parameters	1. L	1. L	1. L	1. L	1. L	1. L
	2. $D_{out}$	2. $D_{out}$	2. $D_{out}$	2. $D_{out}$	2. $D_{out}$	2. $D_{out}$
	3. $D_t$	3. $D_{port}$	3. web	3. web	3. $D_{port}$	3. $D_{port}$
		4. $D_t$	4. $r_1$	4. $r_1$	4. $D_{tip-center}$	4. $D_{tip-center}$
			5. $r_2$	5. $r_2$	5. $D_{tip}$	5. $D_{tip}$
			6. $\eta$	6. $\eta$	6. $D_t$	6. $D_t$
			7. $\xi$	7. $\xi$		7. $L_{slot}$
			8. $D_t$	8. $D_t$		
				9. $L_{star}$		

Table 3.2 Continuous Parameters of Different Grain Types

<b>End Burning, n=3</b>	
Grain length	L
Outer diameter	$D_{out}$
Nozzle throat diameter	$D_t$
<b>Internal Burning Tube, n=4</b>	
Grain length	L
Outer diameter	$D_{out}$
Port diameter	$D_{port}$
Nozzle throat diameter	$D_t$
<b>Star, n=8</b>	
Grain length	L
Outer diameter	$D_{out}$
Web thickness	w
Fillet radius	$r_1$
Cusp radius	$r_2$
Star point semi angle	$\eta$
Star angle	$\xi$
Nozzle throat diameter	$D_t$
<b>Slot, n=6</b>	
Grain length	L
Outer diameter	$D_{out}$
Port diameter	$D_{port}$
Tip-center diameter	$D_{tip-center}$
Tip diameter	$D_{tip}$
Nozzle throat diameter	$D_t$

User defines which grain type will be used and if slot or star grain is selected which number of slot or star points (N) will be tried to the program. For each combination of selected grain types and N, optimization tool runs and finds an

optimum. Then the optimum points are compared and the best one is output as the optimized solution.

An initial guess (grain type, parameters of grain geometry and nozzle throat diameter), is supplied to the program by the user. Upper and lower bounds of the continuous parameters (geometric constraints, such as maximum and minimum outer diameter that the optimization program can try) are also supplied by the user

## **3.2 OPTIMIZER**

The OPTIMIZER uses a heuristic, gradient-free optimization method, the Complex Method developed by Box [29]. The optimization subroutine BC POL from IMSL Math library of FORTRAN 90 is utilized.

### **3.2.1 Complex Method**

Complex Method is a derivative-free, direct search method. A goal in this project is to find the global optimum of a nonsmooth function. It should be obvious that by using a minimization technique which does not use gradients we may actually reach a solution. The complex method has some properties which give it the potential to find the global optimum. This will be discussed below.

Complex Method is a variation of Simplex Method, which was first devised by Spendley et al. [33]. Later Nelder and Mead in 1965 [34] [35] proposed the Extended Simplex Method. Box then developed his own method in order to deal with constrained optimization problems, and called it the Complex Method [16]. Complex method is essentially a modification of Simplex Method for constrained optimization.

The optimization problem to be solved can be stated as follows:

$$\begin{aligned} & \min_{\vec{x} \in R^n} f(\vec{x}) & (3.1) \\ & \text{subject to } \vec{l} \leq \vec{x} \leq \vec{u} \end{aligned}$$

where  $\vec{l}$  is a vector of length  $n$  (number of parameters) containing the lower bounds on variables and  $\vec{u}$  is a vector of length  $n$  containing the upper bounds on variables

Complex Method constructs an initial simplex with  $2n$  nodes, or vertices to solve an optimization problem of  $n$  variables (Figure 3.2 depicts the construction of simplex with  $n+1$  nodes). Each nodes of the simplex represents a set of design parameters, either specified by user or generated randomly without violating constraint equations[35]. Objective function value is evaluated for each node, and then compared with the function value of other nodes to find the worst one. Then this worst node is replaced with a new better one.

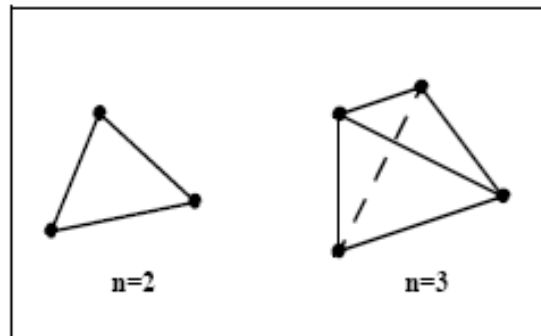


Figure 3.2 Illustration of a Simplex in Two and Three Dimensions [12]

The iterative procedure of the Complex Method is mainly composed of two actions: expansion and contraction. The “worst-valued” node, or the node of the simplex with the largest function value, is eliminated. Then a new node is located away from the old (worst) node with respect to the centroid of other nodes with a reflection factor. Box [16] suggested a reflection factor of 1.3. Since the reflection factor is greater than one, this procedure is called expansion. After the expansion process, the new node is checked for its validity [35]. *“If it violates any constraint*

*equations, or its function value is still the largest, suggesting that the new node is not better than the old one, a midway node will be located to replace the new node with a reflection factor of 0.5, as suggested by Box” [35]. Since the reflection factor is less than one, this procedure is called contraction. The simplex keeps contracting until the new node fulfills all constraint equations and the new node has a smaller function value than the old one. At the end of this iteration attempt a new simplex, with one node improved, is generated. [35]*

The iteration procedure continues until some convergence criteria defined at the beginning of the iteration is reached. And the best node of the last simplex of iteration will be the optimum..

### 3.2.2 BCPOL Subroutine of IMSL

BCPOL/DBCPOL (single/double precision)) subroutine of IMSL library minimizes a function of n variables subject to bounds on the variables using complex algorithm. In this study double precision DBCPOL is used

DBCPOL repeats the iteration of complex algorithm until the maximum number of allowed function evaluations, defined by the user, is reached or one of the following stopping criteria is satisfied:

Criterion 1:

$$f_{\text{best}} - f_{\text{worst}} \leq \epsilon_f (1 + |f_{\text{best}}|) \quad (3.2)$$

Criterion 2:

$$\sum_{i=1}^{2n} \left( f(x_i) - \frac{\sum_{j=1}^{2n} f_j}{2n} \right)^2 \leq \epsilon_f \quad (3.3)$$

where  $\varepsilon_f$  is a user defined tolerance

### 3.3 BURNBACK

At each iteration OPTIMIZER outputs a new iteration point that is a set of design variables; grain geometry parameters and nozzle throat diameter. For these grain geometry parameters, burnback analysis of the grain is performed by the BURNBACK subprogram. Output of these subprogram is web vs. burn area information; web burnt vs. burn area at each burn time.

The output of BURNBACK subprogram is organized in a file that can be directly used as an input file for the internal ballistic program.

#### 3.3.1 Burnback of End-Burning Grain

For end-burning grain type burnback analysis is very straightforward. Initial burn area is calculated analytically as follows;

$$A_b = \frac{\pi D_{out}^2}{4} \quad (3.4)$$

By its very nature, burn area of the end burning grain does not change during the burn time. Therefore initial burn area calculated by using equation 3.4 is constant during the motor operation.

#### 3.3.2 Burnback of Internal Burning Grain

Initial burn area of the internal burning tube grain is calculated analytically as follows;

$$A_b = 2\pi \frac{D_{out}^2 - D_{port}^2}{4} + \pi D_{port} L \quad (3.5)$$

where head and aft ends of the grain are assumed to be unrestricted. If the end areas are defined to be restricted then the first term of the above equation vanishes. For every burn step, the dimensional parameters are adapted with web burnt and the burning surface is calculated again by using the above formula.

### **3.3.3 Burnback of Star and Star-Tube Grain**

For star grain geometry, the analytical burnback methodology presented by Ricciardi [26] is used. Ricciardi presented that based on different geometric evolutions of the star during the web combustion, 16 configurations can be recognized: 8 with convex points and 8 with concave points. Analyzing the geometric evolutions of these 16 configurations, some web intervals were identified, named zones, in which burning surface can be evaluated analytically during the web consumption. For each different zone Ricciardi defines all the geometric relationships used to calculate burning surface as a function of web burnt. A pre-developed computer code utilizing Ricciardi's methodology is used in this study.

Star-tube grain geometry is a combination of star and internal burning tube geometries. Therefore burnback analysis of star-tube geometry is performed as the summation of burn areas evaluated for star and internal burning tube geometries.

### **3.3.4 Burnback of Slot and Slot-Tube Grain**

Since the slot grain is essentially a special case of the concave star grain, same methodology and the computer code used in star grain is valid for slot grain burnback analysis.

Slot-tube grain geometry is a combination of slot and internal burning tube geometries. Therefore burnback analysis of slot-tube geometry is performed as the summation of burn areas evaluated for slot and internal burning tube geometries.

### 3.4 BALLISTICS SOLVER

For the performance prediction of rocket motor, a 0-Dimensional internal ballistics solver is developed and used. This program calculates the pressure-time and thrust-time history of the rocket motor, with inputs of web vs. burn area data, thermo chemical properties of the propellant, nozzle dimensions and performance efficiencies.

#### 3.4.1 Assumptions

Main assumptions of the program are as follows [37]:

1. The combustion gases are ideal gases
2. Burning rate of the propellant follows the empirical correlation  $r_b = aP_c^{n_b}$  from zero to maximum pressure
3. Combustion gas properties throughout the motor is constant.
4. Effects of transient mass addition and erosive burning can be neglected.
5. The chamber gases have negligible inertia
6. Propellant burn rate may be corrected for ambient temperate of the propellant by the relation:

$$r_b = r_b(T_{ref}) \cdot \exp(0.01 \cdot \sigma_p \cdot (T - T_{ref})) \quad (3.6)$$

7. The properties of the gases in the chamber can be found by using weighted averages.

### 3.4.2 Governing Equations

For a radial burning solid rocket motor with subsonic flow ( $M < 1.0$ ), it can be assumed that the properties of gases are constant ( $d(\ )/dx = 0$ ) along the grain length. The total pressure at the throat of the nozzle is also assumed to be equal to the chamber pressure.

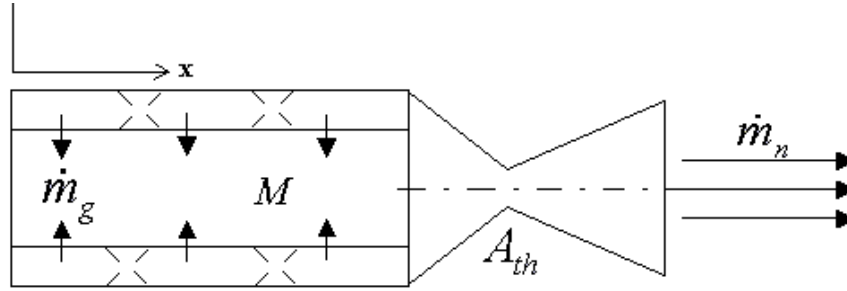


Figure 3.3 Zero-dimensional SRM Conservative Relations [28]

The conservation of mass for isentropic flow can be written as

$$\dot{m}_g = \frac{dM}{dt} + \dot{m}_n \quad (3.7)$$

where  $\dot{m}_g$  is the rate of mass addition by burning propellant,  $\frac{dM}{dt}$  is the rate of change of stored mass in the combustion chamber and  $\dot{m}_n$  is the rate of mass flow through the nozzle. Since in almost all applications nozzle closures are used,  $\dot{m}_n = 0$  until the pressure in the chamber reaches the closure blowout pressure [37].

The rate of mass generation is calculated by the relation

$$\dot{m}_g = \rho_p A_b r_b = \rho_p A_b a P_c^{n_b} \quad (3.8)$$

where  $\rho_p$  is the propellant density and  $A_b$  is the burn area of the grain at that instant. The mass flow through the nozzle is calculated by the relation

$$\dot{m}_n = \frac{P_c A_t}{C^*} \quad (3.9)$$

where  $P_c$  is the chamber pressure,  $A_t$  is the throat area and  $C^*$  is the characteristic speed of the propellant. The throat area may change due to erosion of the nozzle insulation material and the characteristic speed is a function of chamber pressure.

The rate of change of mass stored in the chamber is given by the relation

$$\frac{dM}{dt} = \frac{d(\rho v)}{dt} = \rho \frac{dv}{dt} + v \frac{d\rho}{dt} \quad (3.10)$$

where  $\rho$  is the gas density and  $v$  is the gas volume.

Combining these equations, Equation (3.1) can be re-written as [37]

$$\frac{dP_c}{dt} = \frac{1}{v(t)} \left[ RT_c \left( \rho_p A_b(t) a P_c^{n_{rb}} - \frac{P_c A_t g_0}{C^*} \right) - P_c \frac{dv}{dt} \right] \quad (3.11)$$

where  $\frac{dv}{dt} = r_b A_b$ . Equation (3.5) is integrated with infinitesimal time steps as the propellant burns in order to obtain chamber pressure at these infinitesimal time steps.

Using the chamber pressure, nozzle exit pressure is evaluated by the equation 2.1. And then the thrust coefficient  $C_f$  is calculated by using the equation 2.3.

The thrust is then calculated by the following relation,

$$F(t) = C_f P_c(t) A_t(t) C_d \quad (3.12)$$

where  $C_d$  is the divergence loss coefficient. As seen in the above equation thrust is directly proportional to  $C_f$  and therefore proportional to nozzle exit pressure  $P_e$ . Nozzle exit area is the primary parameter that defines the exit pressure (thrust has been defined in terms of nozzle exit conditions in equation 2.9). Therefore thrust of the rocket motor is highly dependent on nozzle exit area or the expansion ratio

Optimum expansion is obtained when nozzle exit pressure is equal to ambient pressure. To be on the safe side designers choose  $P_e$  as 1.5 atm or 2 atm.

During the design process essentially in optimization, designers deal with a wide variety of chamber pressure and nozzle throat diameter. For each design attempt the nozzle exit area that gives the optimum expansion must be found. Therefore an automated procedure for finding the best nozzle exit area for each design is needed.

A subroutine that calculates desired nozzle exit area depending on the user preference is added to BALLISTIC SOLVER. After the chamber pressure at infinitesimal time steps is calculated by equation 3.5, this subroutine evaluates the average chamber pressure during the burn time of motor. For this average chamber pressure, nozzle exit area that gives the desired exit pressure is calculated by using the below equations.

$$Me = \sqrt{\frac{2}{k-1} \cdot \left[ \left( \frac{P_c}{P_e} \right)^{\frac{k-1}{k}} - 1 \right]} \quad (3.13)$$

$$\frac{A_e}{A_t} = \frac{1}{M_e} \left\{ \frac{2}{k+1} \left[ 1 + \frac{k-1}{2} M^2 \right] \right\}^{\frac{k+1}{2(k-1)}} \quad (3.14)$$

User may prefer to have constant nozzle exit area or prefer that the program calculate the best nozzle exit area for each design.

### 3.5 OBJECT

The OBJECT subprogram calculates the objective function to be optimized (minimized).

For the rocket motors, mission requirements can usually be simplified to the thrust time history of the rocket motor with some geometrical constraints. Rocket motor designer tries to find the best design in order to achieve the desired thrust-time curve. For this reason, the Optimization tool developed in this study tries to find best designs with thrust-time curve that fit the desired thrust-time history.

Therefore the object function to be minimized is defined as how much the current iteration thrust-time curve different than the desired one. It is typically summation of the squares of differences between the desired and computed thrust values at specified times during motor operation divided by average desired thrust and total number of data. It can be formulated as follows,

$$\text{Object.Function} = \frac{\sqrt{\sum_{i=0}^j (F_{\text{desired}} - F_{\text{iteration}})^2}}{j \cdot F_{\text{desired\_avg}}}$$

Where j depends on the time increment of above calculation and maximum of the burn-times of desired and iterated thrust-time curves.

In order to discourage unrealistic designs maximum chamber pressure and propellant mass constraints are enforced by penalty functions. Main idea of the penalty function method is adding a term to the objective function that prescribes a high cost for violation of the constraints. Constraints are specified by the user as maximum chamber pressure and maximum propellant weight.

If the iterated solution has a higher chamber pressure that violates the predefined pressure constraint, the following penalty term is added to the object function;

$$\left( 10 \frac{P_{c_{\max}} - P_{c_{\max\_constr\ int}}}{P_{c_{\max\_constr\ int}}} + 1 \right)^{10} \quad (3.15)$$

If the iterated solution has a higher propellant mass that violates the predefined mass constraint, the following penalty term is added to the object function;

$$\left( 10 \frac{mp - mp_{constr\ int}}{mp_{constr\ int}} + 1 \right)^{10} \quad (3.16)$$

This program calculates and outputs the objective function. This information is then passed to the OPTIMIZER.

## **CHAPTER 4**

### **VALIDATION**

In this section, results obtained for the validation of the optimization tool will be presented. Known solutions, test motor firings and predesigned motor data are used for comparison.

#### **4.1 VALIDATION OF 0-D BALLISTIC SOLVER**

Burnback analysis methods are validated previously. Therefore test cases present in this section are used in order to validate the zero-dimensional ballistic solver.

##### **4.1.1 Tubular Grain Performance Prediction**

Static firing test results of a test motor having tubular propellant grain geometry with two burning ends, named here after “Tubular Motor” TM is used for validation. The grain geometry which is given in Figure 4.1 produces a neutral burning profile (little change in thrust during burning time). Nondimensionalized geometric parameters with respect to the nozzle throat diameter of TM are given in Table 4.1.

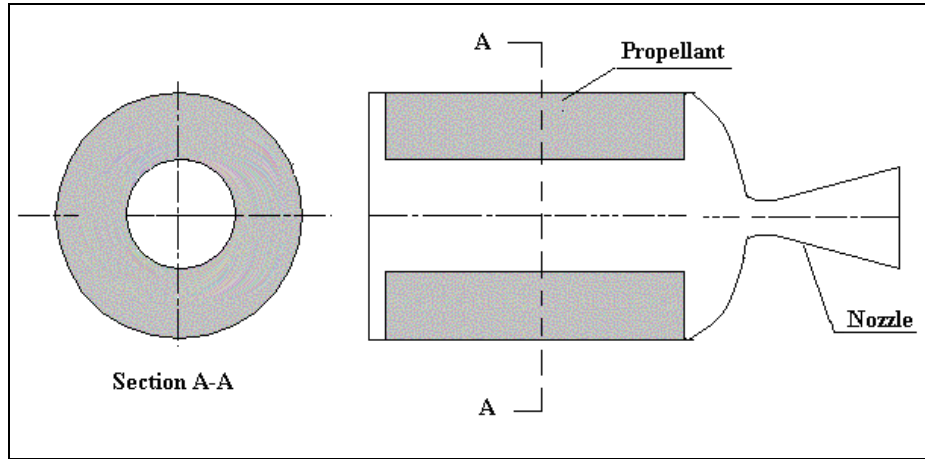


Figure 4.1 Tubular Motor

Table 4.1 Geometric Parameters of Tubular Motor, Nondimensionalized Using the Throat Diameter

Grain length, $L/D_t$	10.6
Grain Outer diameter, $D_{out}/D_t$	5.5
Port diameter, $D_{out}/D_t$	2.8
Nozzle throat diameter, $D_t/D_t$	1.0
Nozzle exit diameter, $D_e/D_t$	2.3

For a fixed propellant type the thrust-time curve of TM at  $-40^\circ\text{C}$  propellant temperature is obtained from zero-dimensional ballistic solver and it is compared with  $-40^\circ\text{C}$  static firing test as shown Figure 4.2 (thrust is normalized with respect to  $F_{max}$  and time is normalized with respect to maximum firing time in Figure 4.2).

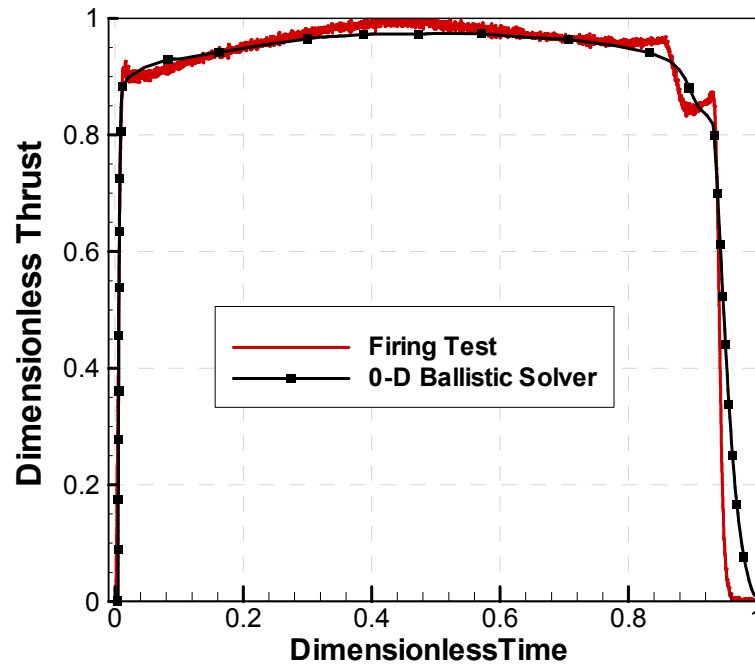


Figure 4.2 Comparison of Thrust-Time Histories of 0-D Ballistic Solver and Firing Test for TM

In order to understand how close ballistic solver estimates the thrust of the motor, objective function is calculated. Here firing test result is the objective thrust-time history and ballistic solver result is the estimated one. Object function is calculated to be 6.07 %.

#### 4.1.2 Star Grain Performance Prediction

Static firing test results of a motor having star grain geometry with 6 star points, named here after “Star Motor” SM is used for validation. Dimensionless geometric parameters of SM are given in Table 4.2

Table 4.2 Dimensionless Geometric Parameters of Star Motor (SM)

Grain length, $L/D_t$	18.8
Outer diameter, $D_{out}/D_t$	3.55
Web thickness, $w/w$	1.00
Fillet radius, $r_1/w$	0.27
Cusp radius, $r_2/w$	0.18
Star point semi angle, $\eta/w$	3.27
Star angle, $\xi/w$	2.27
Nozzle throat diameter, $D_t/D_t$	1.00

The thrust-time curve of SM at +60°C propellant temperature is obtained from zero-dimensional ballistic solver and it is compared with +60°C static firing test as shown in Figure 4.3 (thrust is normalized with respect to  $F_{max}$  and time is normalized with respect to maximum firing time in Figure 4.3).

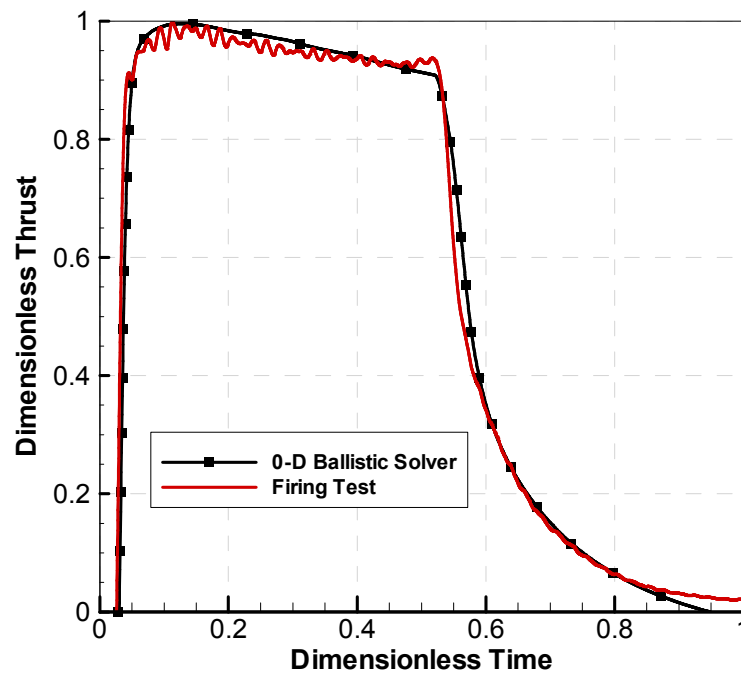


Figure 4.3 Comparison of Thrust-Time Histories of 0-D Ballistic Solver and Firing Test of SM

In order to understand how close ballistic solver estimates the thrust of the motor, objective function is calculated. Here firing test result is the objective thrust-time history and ballistic solver result is the estimated one. Object function is calculated as 5.91 %.

## **4.2 VALIDATION OF OPTIMIZATION TOOL WITH KNOWN SOLUTIONS**

In order to validate the optimization tool, known thrust-time curve of specified grain types are defined to the optimization tool as the objective. An initial guess of the grain parameters far away from the known solution and bounds on the variables are defined to the optimization tool. Optimized solutions are compared with the known, actual, solution of the objective function.

### **4.2.1 Star Grain Optimization**

Star Motor (SM) grain and nozzle properties, given in section 4.1.2, are defined to the zero-dimensional ballistic solver and its thrust-time curve is obtained. This thrust-time history is defined to the optimization tool as the objective (desired) thrust-time.

An initial guess and bounds of the variables are defined as shown in Table 4.3. Only 6 star point geometries are chosen for the optimization. Convergence tolerance for optimization algorithm is defined as  $5 \times 10^{-7}$ . In this test case program converges after 1081 function evaluations and outputs the optimum solution shown in Table 4.3. Values in Table 4.3 are nondimensionalized with SM grain dimensions. Difference between optimized solution and SM grain dimensions is also given in Table 4.3. All the parameters except fillet radius is optimized to the actual solution (SM) with a difference less than 1 percent.

Table 4.3 Initial Guess and Bounds of Parameters of Optimization, SM Grain Dimensions and Optimized Solution

<b>Parameter</b>	<b>Initial Guess</b>	<b>Lower Bound</b>	<b>Upper Bound</b>	<b>SM Grain</b>	<b>Optimized Values</b>	<b>Difference (%)</b>
Grain length, $L / L_{SM}$	0.90	0.90	1.14	1.00	1.00	0.22
Outer diameter, $D_{out} / D_{out,SM}$	1.33	0.84	1.45	1.00	0.99	0.41
Web thickness, $w / w_{SM}$	0.73	0.73	1.82	1.00	1.00	0.91
Fillet radius, $r_1 / r_{1,SM}$	0.83	0.50	1.17	1.00	0.97	3.00
Cusp radius, $r_2 / r_{2,SM}$	1.25	0.80	1.50	1.00	1.00	0.00
Star point semi angle, $\eta / \eta_{SM}$	0.89	0.83	1.11	1.00	1.00	0.03
Star angle, $\xi / \xi_{SM}$	1.12	0.80	1.20	1.00	1.00	0.12
Throat diameter, $D_t / D_{t,SM}$	1.07	0.64	1.07	1.00	1.00	0.09

Dimensionless initial guess and optimized solution are also shown in Figure 4.4 (thrust is normalized with respect to  $F_{max}$  and time is normalized with respect to maximum firing time in Figure 4.2). As seen in Table 4.3 and in Figure 4.4 optimization tool starts with an initial guess far away from the objective thrust-time curve, but the optimized solution is very close to the objective with less than 1 % difference.

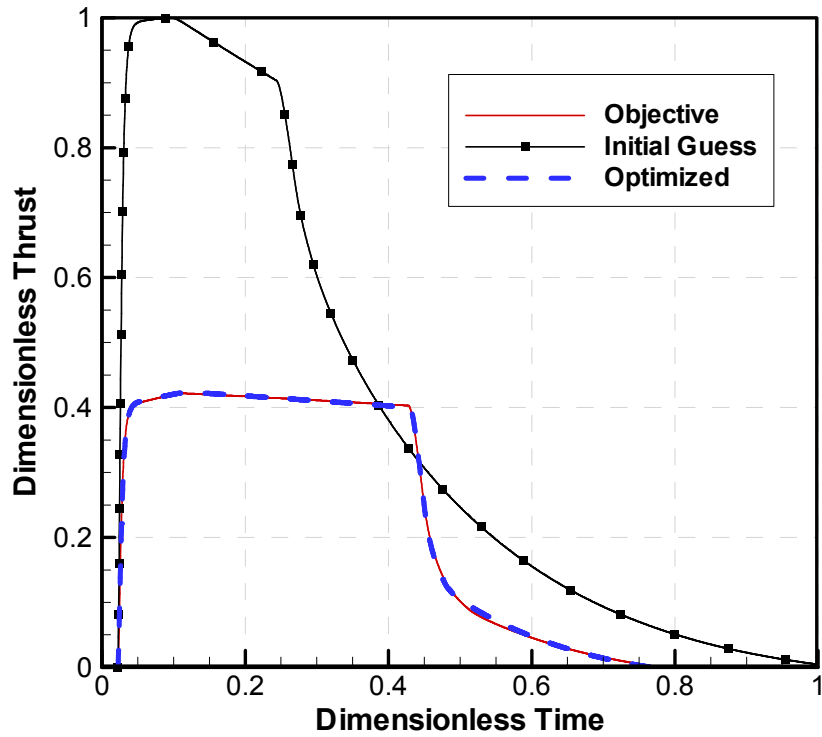


Figure 4.4 Comparison of Thrust-Time histories of Optimized Solution, Initial Guess and Objective for SM

#### 4.2.2 Slot-Tube Grain Optimization

Thrust-time history of a motor having a certain slot-tube grain geometry with 5 slot points, named here after “Slot-Tube Motor” STM is used for validation. Dimensionless geometric parameters of STM are given in Table 4.4

Table 4.4 Dimensionless Geometric Parameters of Slot-Tube Motor (STM)

Grain length, $L/D_t$	44.1
Outer diameter, $D_{out}/D_t$	2.8
Port diameter, $D_{port}/D_{tip}$	9.2
Tip-center diameter, $D_{tip-center}/D_{tip}$	15.8
Tip diameter, $D_{tip}/D_{tip}$	1.0
Nozzle throat diameter, $D_t/D_t$	1.0
Slot length, $L_{slot} / L$	0.2

Slot-Tube Motor (STM) grain and nozzle properties, are defined to the zero-dimensional ballistic solver and its thrust-time curve is obtained. This thrust-time history is defined to the optimization tool as the objective (desired) thrust-time.

An initial guess and bounds of the variables are defined as shown in Table 4.3. Only 5 slot point geometries are chosen for the optimization. Convergence tolerance for optimization algorithm is defined as  $5 \times 10^{-7}$ . For this case program converges after 791 function evaluations and outputs the optimum solution shown in Table 4.5. Convergence is assumed when the objective function value is 0.003.

Table 4.5 Initial Guess and Bounds of Parameters of Optimization, STM Grain Dimensions and Optimized Solution

<b>Parameter</b>	<b>Initial Guess</b>	<b>Lower Bound</b>	<b>Upper Bound</b>	<b>STM Grain</b>	<b>Optimized Values</b>	<b>Difference (%)</b>
Grain length, $L / L_{STM}$	1.05	0.98	1.05	1.00	0.99	0.68
Outer diameter, $D_{out} / D_{out,STM}$	1.11	0.90	1.13	1.00	0.96	0.47
Port diameter, $D_{port} / D_{port,STM}$	1.49	0.96	1.53	1.00	0.97	3.32
Tip-center diameter, $D_{tip-center} / D_{tip-center,STM}$	1.19	0.89	1.19	1.00	1.00	0.05
Tip diameter, $D_{tip} / D_{tip,STM}$	1.40	0.60	1.60	1.00	0.80	19.8
Throat diameter, $D_t / D_{t,STM}$	1.05	0.72	1.05	1.00	0.98	2.06
Slot length, $L_{slot} / L_{slot,STM}$	1.42	0.81	1.45	1.00	1.02	1.45

Difference between optimized solution and STM grain dimensions is also given in Table 4.3 as percent difference. Nondimensionalized initial guess and optimized solution are shown in Figure 4.5 (thrust is normalized with respect to  $F_{max}$  and time is normalized with respect to maximum firing time in Figure 4.5).

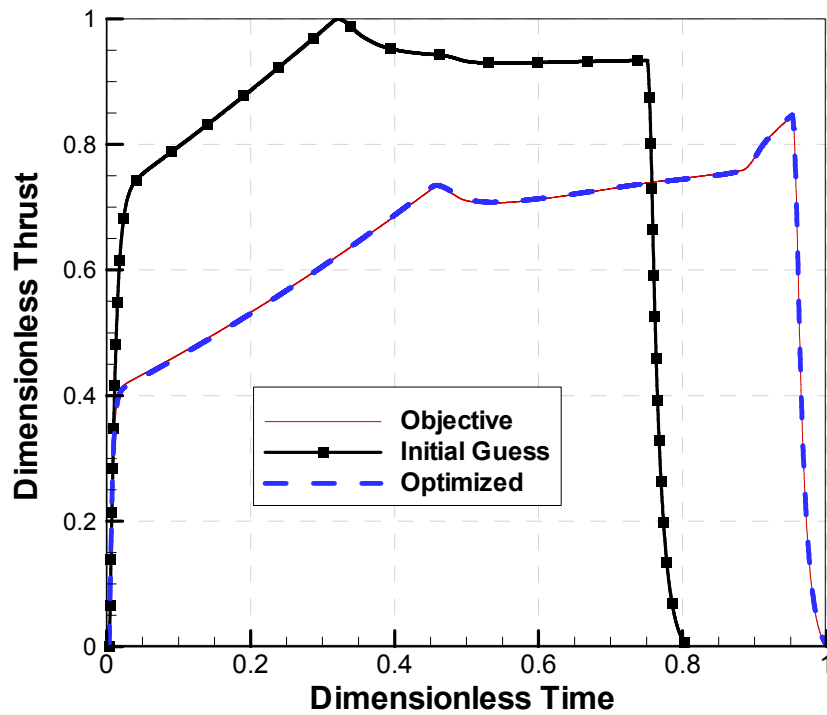


Figure 4.5 Comparison of Thrust-Time histories of Optimized Result, Initial Guess and Objective for STM

As seen in Table 4.5 and in Figure 4.5 optimization tool starts with an initial guess far away from the objective thrust-time curve, but the optimized solution is very close to the objective.

### 4.3 VALIDATION OF OPTIMIZATION TOOL AND COMPARISON WITH PREDESIGNED ROCKET MOTORS

When the mission requirements of a missile or rocket system is considered, these requirements can be simplified to the thrust-time history of the rocket motor. Usually the specification of this thrust-time history is in terms of total thrust and time or average thrust. Typical motor design requirements are shown in Figure 4.6.

In this part of the study an objective similar to these curves is given to the optimization program. Objectives of predesigned rocket motors are implemented and optimized solutions are compared with these rocket motors to see whether the optimization tool gives better designs than the present designs.

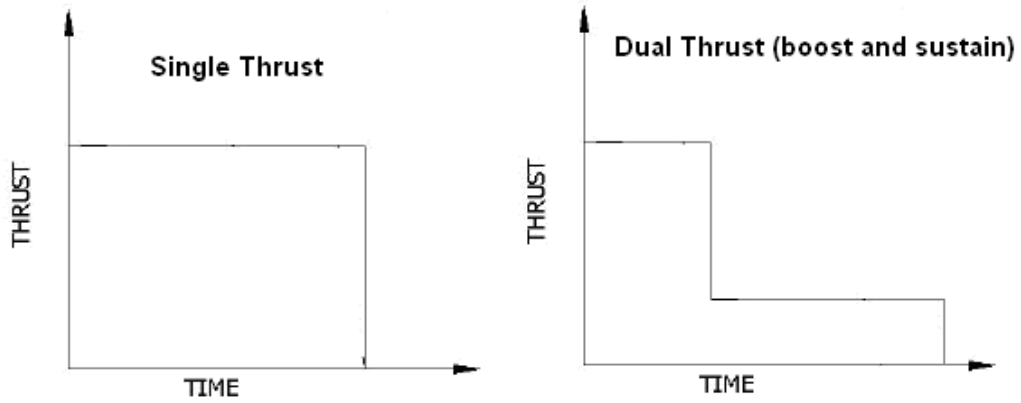


Figure 4.6 Typical Thrust-Time Requirements of Solid Rocket Motors

In order to define objective thrust-time curve, total impulse and average thrust of the actual STM is calculated. And a new thrust time curve that meets these total impulse and average thrust requirements is prepared. as the objective function of the optimization.

#### 4.3.1 Star Grain Optimization

A Star Motor (SM) was previously designed without the aid of any optimization tool, by trial and error and knowledge of experience. The motor has a known star grain configuration with 6 star points, and a known nozzle geometry. Grain and nozzle parameters of this motor are given in section 4.1.2.

In order to define objective thrust-time curve, total impulse and average thrust of the actual SM is calculated, and a new thrust time curve that meets these total

impulse and average thrust requirements is prepared as the objective of the optimization.

As seen in Figure 4.7, SM thrust has a slow decrease after the time is 0.45. This part of the curve, called the sliver region, is almost useless due to the inefficient burning of the propellant. Sliver is an inherent characteristic of star geometry but the amount depends on the specific design. Any design having relatively small sliver region is more acceptable. Therefore average thrust of SM is calculated up to time 0.45 and the remaining part of the curve is discarded. Implementing this average thrust, the objective thrust-time curve of this test case is defined as in Figure 4.7 (thrust is normalized with respect to  $F_{max}$  and time is normalized with respect to maximum firing time in Figure 4.7).

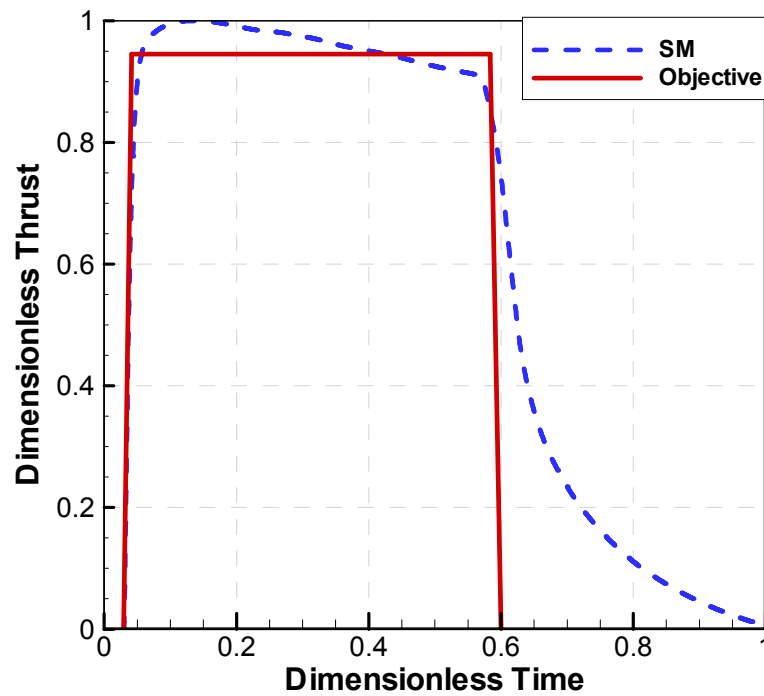


Figure 4.7 Objective Thrust-Time Prepared for Optimization and SM Thrust-Time Curve

For this test case an initial guess and bounds on the variables are defined as shown in Table 4.6. Values in Table 4.6 are nondimensionalized with the SM grain parameters. Grain length and outer diameter bounds come from the SM design. Designer of the SM had these constraints on grain length and outer diameter. Therefore these constraints are given to the optimization tool without any change. But the bounds of the other parameters are now chosen arbitrarily considering producibility issues.

Maximum chamber pressure is constrained to be 3000 Psi and propellant weight is constrained to be 4 kg using the penalty functions explained in Chapter 3.5. Star geometries of  $N=4-8$  are chosen for the optimization. In this test case the exact solution is not known prior to optimization. Optimization tool is expected to give a better design solution compared to the original SM

Table 4.6 Dimensionless Initial Guess Parameters and Bounds of Star Grain Optimization

<b>Parameter</b>	<b>Initial Guess</b>	<b>Lower Bound</b>	<b>Upper Bound</b>
Grain length, $L / L_{SM}$	1.05	0.96	1.05
Outer diameter, $D_{out} / D_{out,SM}$	0.96	0.96	1.02
Web thickness, $w / w_{SM}$	0.73	0.73	1.27
Fillet radius, $r_1 / r_{1,SM}$	1.50	0.50	1.50
Cusp radius, $r_2 / r_{2,SM}$	1.25	0.75	2.25
Star point semi angle, $\eta / \eta_{SM}$	0.83	0.83	1.11
Star angle, $\xi / \xi_{SM}$	1.12	0.80	1.20
Nozzle throat diameter, $D_t / D_{t,SM}$	0.94	0.77	1.54

Initial guess thrust-time curves compared to objective thrust-time curve are shown in Figure 4.8 (thrust is nondimensionalized with respect to  $F_{max}$  of initial guesses and time is nondimensionalized with respect to maximum firing time of initial guesses in Figure 4.8).

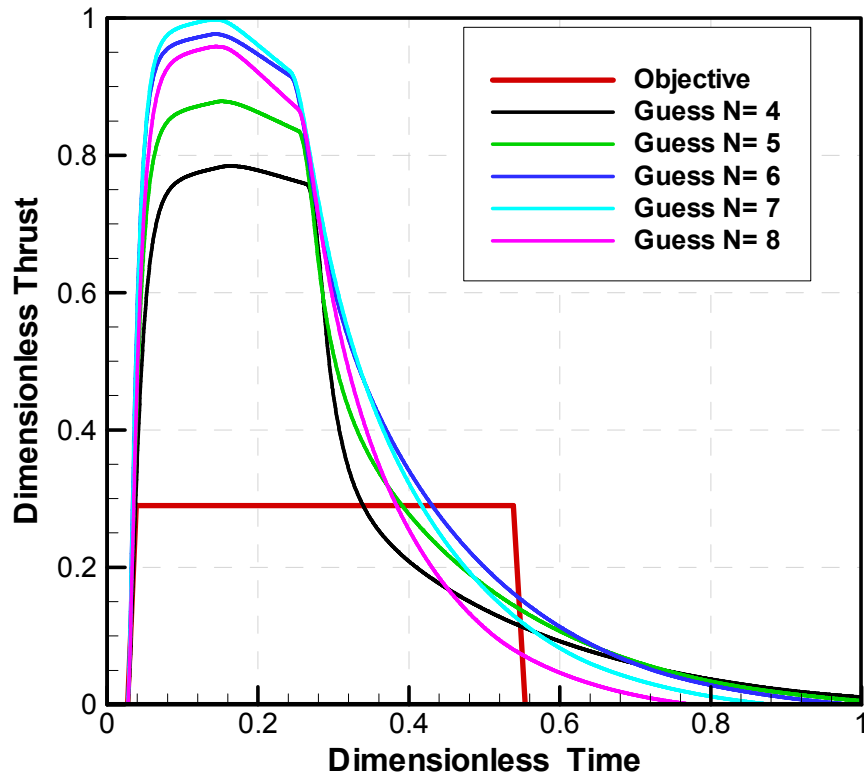


Figure 4.8 Comparison of Thrust-Time histories of Initial Guess for Different Number of Stars and Objective for Star Optimization

The convergence tolerance used for optimization algorithm is  $5 \times 10^{-7}$ . Optimization algorithm converged for each star geometry, program outputs for different star geometries are shown in Figure 4.9 also in Table 4.7 (thrust is nondimensionalized with respect to  $F_{max}$  and time is nondimensionalized with respect to maximum firing time in Figure 4.9, values in Table 4.7 are nondimensionalized with SM grain dimensions). Star Motor is also shown in Figure 4.9 and in Table 4.7 for comparison.

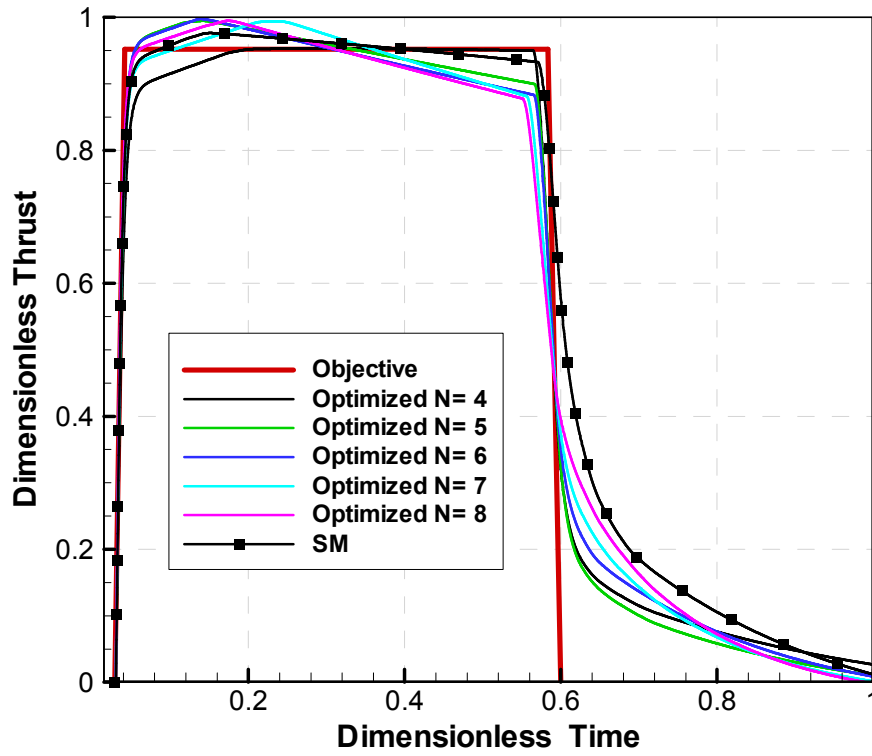


Figure 4.9 Comparison of Thrust-Time Histories of Initial Guesses and Optimized Results for Star Grain Optimization

Table 4.7 Dimensionless Optimized Results for Star Grain

Parameters	Optimized Star Geometries					SM
	N = 4	N = 5	N = 6	N = 7	N = 8	N = 6
Grain length, $L / L_{SM}$	1.02	1.05	1.03	1.01	1.00	1.00
Outer diameter, $D_{out} / D_{out,SM}$	1.02	1.02	1.01	1.01	0.91	1.00
Web thickness, $w / w_{SM}$	0.94	0.90	0.91	0.90	0.89	1.00
Fillet radius, $r_1 / r_{1,SM}$	0.73	0.73	0.73	0.83	0.77	1.00
Cusp radius, $r_2 / r_{2,SM}$	1.40	0.85	0.95	1.80	1.25	1.00
Star point semi angle, $\eta / \eta_{SM}$	0.99	0.91	0.95	0.96	1.04	1.00
Star angle, $\xi / \xi_{SM}$	0.92	0.80	0.80	0.80	0.80	1.00
Throat diameter, $D_t / D_{t,SM}$	1.03	1.09	1.07	1.06	1.06	1.00
Objective Function (%)	6.9	6.5	8.2	9.3	10.6	11.2

Objective function value that is minimized at the end of optimization (as described in section 3.5) is also given in Table 4.7 for each star geometry. For comparison objective function is calculated for the actual SM geometry and it is found to be 11.2 % for this objective thrust-time curve.

All of the optimized star grain geometries have a better curve fit with the objective thrust-time curve than the actual motor SM. The minimum function value is obtained for the star geometry with 5 star points. Therefore this 5 star grain geometry has a thrust-time curve more close to the objective thrust-time curve than all the other star grains within the specified bounds and constraints.

### **4.3.2 Slot-Tube Grain Optimization**

Slot-Tube Motor (STM) was previously designed without the aid of any optimization tool, by trial and error and based on experience. The motor has a known slot-tube grain configuration with 5 slot points, and a known nozzle geometry. Grain and nozzle parameters of this motor are given in section 4.2.2.

In order to define objective thrust-time curve, total impulse and average thrust of the actual STM is calculated, and a new thrust time curve that meets these total impulse and burn time requirements is prepared as the objective of the optimization. Comparison of the objective and STM thrust-time curves is shown in Figure 4.10 (thrust is nondimensionalized with respect to  $F_{max}$  and time is nondimensionalized with respect to maximum firing time in Figure 4.10).

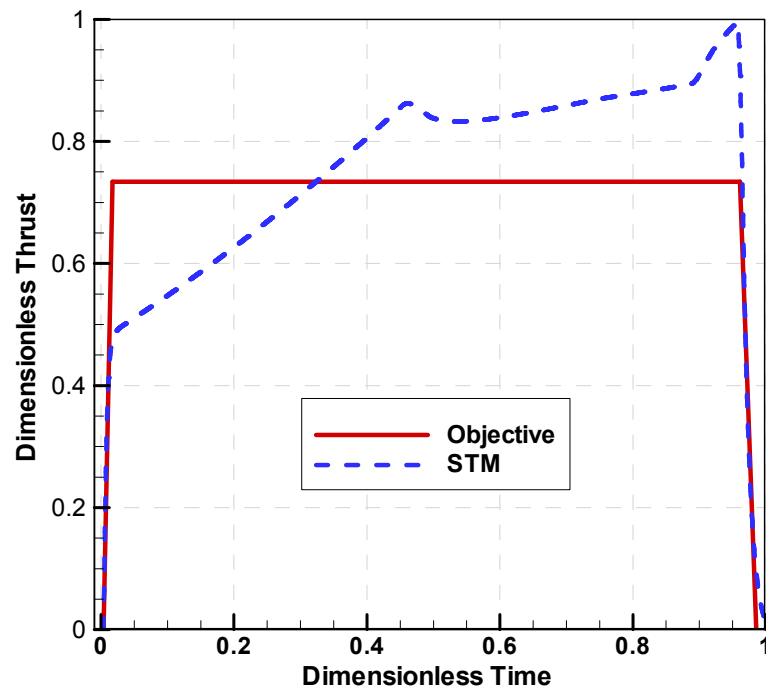


Figure 4.10 Objective Thrust-Time Prepared for Optimization and Original STM's Thrust-Time Curve

For this test case an initial guess and bounds on the variables are defined as shown in Table 4.8. Values in Table 4.8 are nondimensionalized with the STM grain parameters. Grain length and outer diameter were fixed for the STM design. Therefore grain length and outer diameter is not variable for this optimization test case. Also the nozzle exit diameter must be lower than a certain value. All these constraints are defined in the optimization process. But the bounds of the other parameters are now chosen arbitrarily considering producibility issues. Also maximum chamber pressure is constrained to be 3000 Psi using the penalty functions explained in Chapter 3.5. Slot geometries of N=4-8 are chosen for the optimization.

Table 4.8 Dimensionless Initial Guess Parameters and Bounds of Slot-Tube Grain Optimization

<b>Parameter</b>	<b>Initial Guess</b>	<b>Lower Bound</b>	<b>Upper Bound</b>
Grain length, $L / L_{STM}$	1.00	1.00	1.00
Outer diameter, $D_{out} / D_{out,STM}$	1.00	1.00	1.00
Port diameter, $D_{port} / D_{port,STM}$	1.09	0.83	1.53
Tip-center diameter, $D_{tip-center} / D_{tip-center,STM}$	0.92	0.88	1.17
Tip diameter, $D_{tip} / D_{tip,STM}$	1.20	0.80	1.80
Throat diameter, $D_t / D_{t,SM}$	0.86	0.72	1.08
Slot length, $L_{slot} / L_{slot,STM}$	1.61	0.81	2.10

Initial guess thrust-time curves compared to objective thrust-time curve are shown in Figure 4.11 (thrust is nondimensionalized with respect to  $F_{max}$  of initial guesses and time is nondimensionalized with respect to maximum firing time in Figure 4.11).

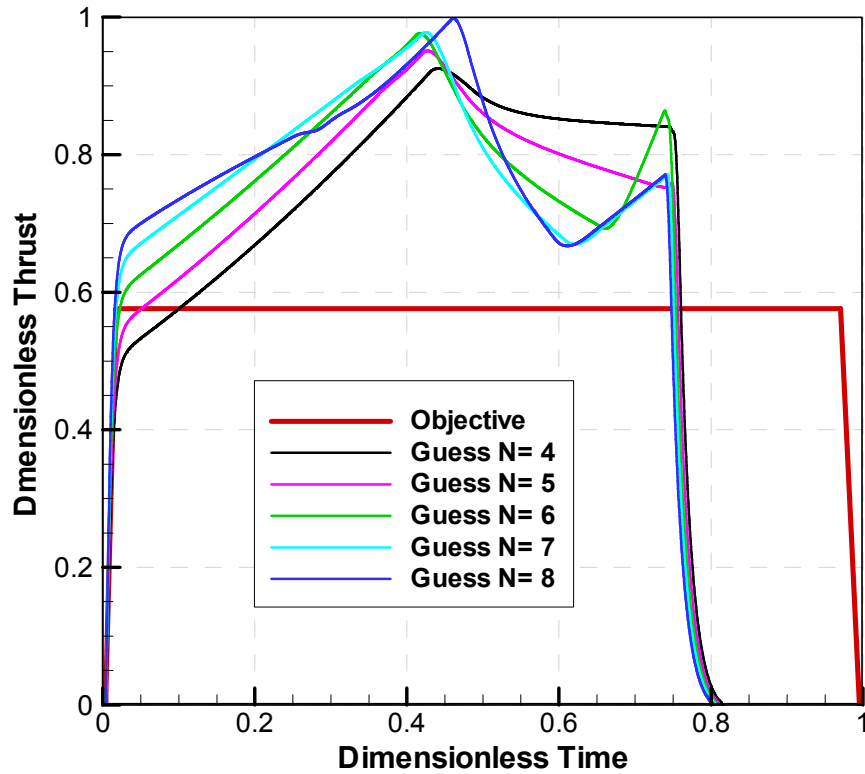


Figure 4.11 Comparison of Thrust-Time histories of Initial Guess for Different Number of Slots and Objective

The convergence tolerance used for optimization algorithm is  $5 \times 10^{-7}$ . Optimization algorithm converged for each slot-tube geometry, program outputs for different slot number geometries are shown in Figure 4.12 and in Table 4.9 (thrust is nondimensionalized with respect to  $F_{\max}$  and time is nondimensionalized with respect to maximum firing time in Figure 4.12, values in Table 4.9 are nondimensionalized with STM grain dimensions). Slot-Tube Motor (SM) is also shown in Figure 4.12 and in Table 4.9 for comparison.

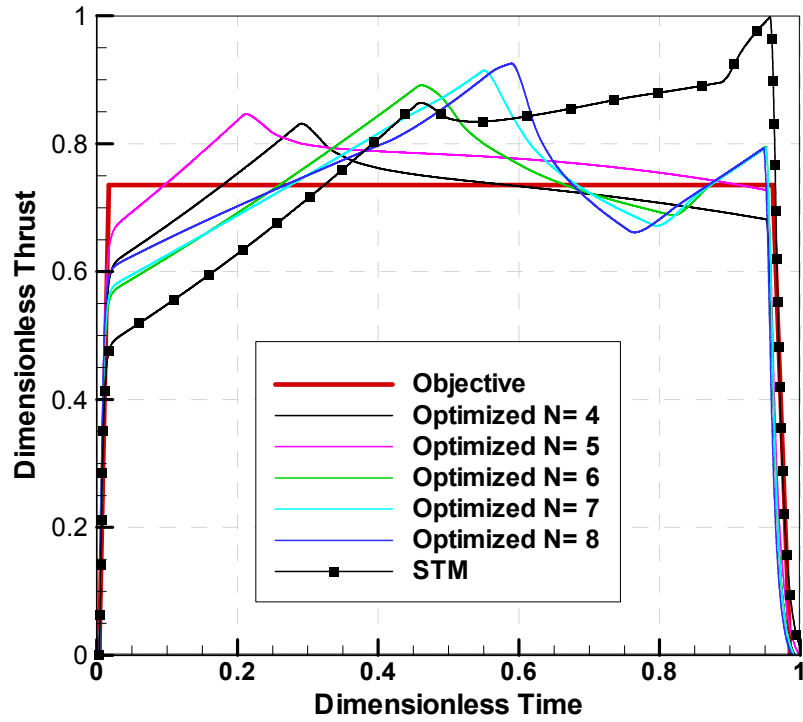


Figure 4.12 Comparison of Thrust-Time histories of Initial Guesses and Optimized Results for Slot-Tube Grain

Table 4.9 Dimensionless Optimized Results for Slot-Tube Grain

Parameters	Optimized Slot-Tube Geometries					STM
	N = 4	N = 5	N = 6	N = 7	N = 8	N = 5
Grain length, $L / L_{STM}$	1.00	1.00	1.00	1.00	1.00	1.00
Outer diameter, $D_{out} / D_{out,STM}$	1.00	1.00	1.00	1.00	1.00	1.00
Port diameter, $D_{port} / D_{port,STM}$	1.09	0.98	1.10	1.10	1.10	1.00
Tip-center diameter, $D_{tip-center} / D_{tip-center,STM}$	1.10	1.16	0.96	0.91	0.90	1.00
Tip diameter, $D_{tip} / D_{tip,STM}$	1.70	1.56	1.14	1.06	0.90	1.00
Throat diameter, $D_t / D_{t,STM}$	1.05	0.98	1.07	1.08	1.08	1.00
Slot length, $L_{slot} / L_{slot,STM}$	1.98	1.52	1.39	1.39	1.39	1.00
Objective Function (%)	6.2	6.7	10.5	11.4	11.1	19.8

Objective function value that is minimized at the end of optimization (as described in section 3.5) is also given in Table 4.7 for each slot-tube geometry. The minimum function value is obtained for slot-tube geometry with 4 slot points. For comparison objective function is calculated for the STM geometry and it is found to be 19.8 % for this objective thrust-time curve.

All of the optimized grain geometries have a better curve fit with the objective thrust-time curve than the actual motor STM. The minimum function value is obtained for slot-tube geometry with 4 slot points. Therefore this 4 slot grain geometry has a thrust-time curve more close to the objective thrust-time curve than all the other grains within the specified bounds and constraints.

## CHAPTER 5

### CONCLUSION AND DISCUSSION

The purpose of this study is to develop an internal ballistic design optimization tool for solid rocket motors

An optimization tool for an internal ballistic design of solid rocket motors has been developed and presented. A direct search method Complex algorithm is used in this study. Optimization algorithm changes the grain geometric parameters and nozzle throat diameter finally achieving the optimum results. The main features of the developed code are given below.

Optimization tool developed in this study, involves geometric modeling of the propellant grain, burnback analysis, ballistic performance prediction analysis of rocket motor and the mathematical optimization algorithm. Six types of propellant grain geometries are involved in this study; end burning, internal burning tube, slot, slot-tube, star and star-tube grain geometries. Burnback analysis is conducted by using analytical methods. For the performance prediction of rocket motor, a 0-D internal ballistic solver is developed and used. The objective function that is optimized is summation of the squares of differences between the desired and computed thrust values at specified times during motor operation divided by the average desired thrust and total number of data.

Optimization tool validation is shown by comparing the results with known solutions and predesigned rocket motor results.

For this study;

1. implementation of dual- pulse operating motor or double motor solvers may increase the capability of the optimization tool,
2. implementation of structural design parameters into the optimization algorithms,
3. implementation of stability parameters into the optimization algorithms,

would be the future areas of interest for further research.

## REFERENCES

- [1] Sforzini, Richard H., "*An Automated Approach to Design of Solid Rockets Utilizing a Special Internal Ballistics Model*", AIAA Paper 80-1135, Presented at the AIAA/SAE/ASME 16th Joint Propulsion Conference, June 30-July 2, 1980.
- [2] Anderson, M., Burkhalter, J., and Jenkins, R., "*Multi-Disciplinary Intelligent Systems Approach to Solid Rocket Motor Design, Part I: Single and Dual Goal Optimization*", AIAA 2001-3600, 2001
- [3] Billheimer, J.S., "*Optimization and Design Simulation in Solid Rocket Design*," AIAA 68-488,1968.
- [4] Woltosz, W.S., "*The Application of Numerical Optimization Techniques to Solid-Propellant Rocket Motor Design*", M.S. Thesis, Auburn University, Auburn, Alabama, March 1977.
- [5] Hooke, R., and Jeeves, T.A., "*Direct Search Solution of Numerical and Statistical Problems*", Journal of the Assoc. of Comp. Mac/7., Vol. 8, No. 2, pp. 212-229.
- [6] Foster, W.A., Jr., and Sforzini, R.H., "*Optimization of Solid Rocket Motor Igniter Performance Requirements*", AIAA 78-1016, 1978.
- [7] Swaminathan, V., Madhavan, N.S., "*A Direct Random Search Technique for the Optimization of Propellant Systems*," Indian Institute of Science, The Journal of the Aeronautical Society of India, Vol. 32, No. 1-4, pp. 101-104,1980,
- [8] Clergen, J.B., "*Solid Rocket Motor Conceptual Design - The Development Of A Design Optimization Expert System With A Hypertext User Interface*," AIAA 93-2318,1993
- [9] McCain, J.W., "*A Variable Selection Heuristic for Solid Rocket Motor Design*," The University of Alabama-Huntsville, Dissertation, University Microfilms No. DA9324488

- [10] Nisar, K., Guozhu, L., “*A Hybrid Approach for Design Optimization of Wagon Wheel Grain for SRM*”, AIAA 2008-4893
- [11] Nisar, K., Guozhu, L., “*A Hybrid Optimization Approach for SRM FINOCYL Grain Design*”, Chinese Journal of Aeronautics 21(2008) 481-487
- [12] Ryan A. Fellini., “*Derivative-Free and Global Search Optimization Algorithms in an Object-Oriented Design Framework*”, MS. Thesis Department of Mechanical Engineering and Applied Mechanics, University of Michigan, 1998.
- [13] Gill, P.E, Murray, W., and Wright M.H., “*Practical Optimization*”, London, Academic Press, 1981
- [14] Bairstow, B.K., “*Effectiveness of integration of System-Level Optimization in Concurrent Engineering for Rocket Design*”, MS. Thesis Department of Aeronautics and Astronautics, Massachusetts Institute of Technology, 2004
- [15] Dennis, J.E., Jr., Torczon, V., “*Direct Search Methods on Parallel Machines*,” SIAM Journal on Optimization, Volume 1, No. 4, pp. 448-474, 1991.
- [16] Box, M.J., “*A New Method of Constrained Optimization and a Comparison with other Methods*,” Imperial Chemical Industries Limited, Central Instrument Research Laboratory, Bozdown House, WhitChurch Hill, Nr. Reading, Berks, 1965.
- [17] Jones, D.R., Perttunen, C.D., and Stuckman, B.E., “Lipschitzian Optimization Without the Lipschitz Constant,” Journal of Optimization Theory and Applications, Volume 79, No.1, October, 1993.
- [18] Sutton, G., P., Biblarz, O., “*Rocket Propulsion Elements*”, John Wiley & Sons, 7th edition, 2001,
- [19] [1] Barrere. M, Joumatte. A, Vandenkerckhove. J, “*Rocket Propulsion*”, The Advisory Group for Aeronautical Research and Development of NATO, New York, 1960

- [20] Yıldırım C., “*Analysis of Grain Burnback and Internal Flow In Solid Propellant Rocket Motors in 3- Dimensions*”, Ph. D. Dissertation, Dept. of Mechanical Engineering, METU, 2007.
- [21] Püskülcü G., “*Analysis of 3-D Grain Burnback of Solid Propellant Rocket Motors and Verification with Rocket Motor Tests*”, MS. Thesis, Dept. of Mechanical Engineering, METU 2004
- [22] Davenas A., “*Solid Rocket propulsion Technology*”, 1993
- [23] “*Solid Propellant Grain Design and Internal Ballistics*”, NASA, SP-8076, 1972
- [24] Hartfield, R., Jenkins, R., Burkhalter, J., Foster, W., “*A Review of Analytical Methods for Solid Rocket Motor Grain Analysis*” AIAA 2003-4506, July, 2003
- [25] Barrere, M., Jaumotte, A., Veubeke, B.,and Vandenkerckhove, J., “*Rocket Propulsion*”, Elsevier Publishing Company, Amsterdam, 1960.
- [26] Ricciardi, A., “*Generalized Geometric Analysis of Right Circular Cylindrical Star Perforated and Tapered Grains*”, J.Propulsion Vol. 8, No. 1, Jan-Feb 1992
- [27] U.S. Air Force Astronautics Lab. “*The Solid Propellant Rocket Motor Performance Prediction Computer Program (SPP)*”, AFAL-TR-87-078, 1987
- [28] Toker K.A., “*Three-Dimensional Retarding Walls and Flow in Their Vicinity*”, Ph.D. Thesis Submitted to the Graduate School of Natural and Applied Sciences of the Middle East Technical University, Dec 2004.
- [29] Willcox M. A., Brewster M. Q., Tang K. C., Stewart D. S, “*Solid Propellant Grain Design and Burnback Simulation Using a Minimum Distance Function*”, AIAA-2005-4350, 41st AIAA/ASME/SAE/ASEE Joint Propulsion Conference, Tucson, Arizona, 2005.

- [30] Hejl R. J., Heister S. D., “*Solid Rocket Motor Grain Burnback Analysis Using Adaptive Grids*”, Journal of Propulsion and Power, Vol 11, No 5, pp1006-1012, 1995
- [31] Mashayek F., Ashgriz N., “*Solid Propellant Grain Design by an Interface Reconstruction Technique*”, Journal of Spacecraft and Rockets, Vol 31, No5, pp908-910, 1994
- [32] Zarchan P., Editor-in-chief, “*Tactical Missile Propulsion*”, AIAA, Virginia, 1996
- [33] Spendley W, Hext GR, Himsworth FR. “Sequential applications of simplex designs in optimization and evolutionary operation”. Technometrics 1962;4:441–61.
- [34] Nelder JA, Mead R. “A simplex method for function minimization.” The Comput J 1965;7:308–13.
- [35] Ssu-yuan Hu, Jung-Ho Cheng, “Development of the unlocking mechanisms for the complex method” Computers and Structures 83(2005) 1991–2002
- [36] Bunday BD. Basic optimisation methods. Edward Arnolds 1984:98–102.
- [37] Netzer, D.W, “Propulsion Analysis for Tactical Solid Propellant Rocket Motors”, Lecture Notes, 1990